CON[redacted]AL Report No. BMI-1231 UNCLASSIFIED

C-83 - Reactors - Special Features of Military Package Power Reactors (M-3679, 20th Ed., Rev. 1)

Contract No. W-7405-eng-92

NEUTRON-FLUX MEASUREMENTS IN A FLAT PLATE FUEL ELEMENT

This document is
PUBLICLY RELEASABLE
N. Kinser
Authorizing Official
Date: 2/11/10

by

Walter R. Morgan
James N. Anno, Jr.
Joel W. Chastain, Jr.

Classification cancelled (or changed to UNCLASSIFIED)
Ltr. Fr. Declassification
by authority of Branch Dated 12-3-59
by J. C. Ridenour T.E, date 12-11-59

October 31, 1957

~~RESTRI[redacted]ED DA[redacted]A~~
~~This document conta[redacted]d in the Atomic Energy Act of [redacted] disclosure of its contents in any man[redacted] unauth[redacted] person is prohibited.~~

BATTELLE MEMORIAL INSTITUTE
505 King Avenue
Columbus 1, Ohio

[redacted] UNCLASSIFIED

DISCLAIMER

DISCLAIMER

Portions of this document may be illegible in electronic image products. Images are produced from the best available original document.

TABLE OF CONTENTS

NEUTRON-FLUX MEASUREMENTS IN A FLAT PLATE FUEL ELEMENT

Walter R. Morgan, James N. Anno, Jr., and Joel W. Chastain, Jr.

This report describes the equipment and experiments performed to measure the thermal-neutron-flux distribution in a fuel assembly of an experimental loop mock-up of a gas-cooled reactor at the Battelle Research Reactor (BRR). The loop was located adjacent to the core of the BRR and contained one fuel assembly composed of seven flat fuel plates each containing approximately 29.5 g of uranium-235. The plates consisted of a core 0.050 in. thick of UO_2 dispersed in Type 347 stainless steel and clad on each side with 0.005 in. of Type 347 stainless steel.

The measurements showed that with the present design of the loop system an average thermal-neutron flux of 4.09×10^{12} neutrons/(cm^2)(sec) or a power generation of 45 kw in the assembly can be conveniently obtained. The ratio of the peak thermal-neutron flux to average thermal flux in the entire element was found to be 1.87. At any horizontal cross section, thermal-flux depression from the edge of the element to the center of less than a factor of two was observed for the final loop-core arrangement.

INTRODUCTION

As a part of the materials research effort for the gas-cooled-reactor program, a test loop has been constructed for irradiating test fuel elements in the Battelle Research Reactor (BRR). This loop facility has been designed to test fuel elements under conditions simulating GCRE operation as closely as possible.

The first fuel-specimen type, designated Mark I for reference purposes, is a parallel-plate element. Prior to operation of the loop under operating temperatures and power conditions, it was considered desirable to determine the neutron-flux distribution within the element as it would be under loop test conditions.

This report presents those measurements taken with the Mark I element, which include neutron-flux distribution and flux depression within the element.

DESCRIPTION OF THE APPARATUS

Loop Mock-Up

For the flux-measurement program, a special mock-up of the fuel-element test loop was constructed. This mock-up duplicates the test loop in the vicinity of the reactor core both in dimensions and materials, and for the remainder of this report will be referred to as the loop. Basically, the loop consists of three concentric pipes separated to provide passage of the coolant gas and to provide a "dead" gas layer to serve as insulation. The central pipe is square in cross section and serves as a sleeve for the test fuel element. A sketch of the loop cross section is shown in Figure 1. The loop is suspended vertically on the tower of a movable bridge (referred to as the instrument bridge) spanning the reactor pool. The photograph, Figure 2, shows the towers of the instrument bridge (right) and the reactor bridge (left) with the reactor pool drained and the reactor bridge moved from the normal operating position.

For the irradiations, the reactor bridge is moved into the pocket formed by the beam tubes and the instrument bridge with the loop attached is moved adjacent to the reactor core. A photograph of the loop and the supports which fasten it to the tower of the instrument bridge is shown in Figure 3. The central Inconel sleeve containing the test specimen is attached by a rod to a threaded plug at the top of the loop. Figure 4 shows the test fuel element, Inconel sleeve, and threaded plug prior to assembly and insertion into the loop.

Test Fuel Element

The Mark I fuel element is 24 in. long and is composed of seven flat fuel plates brazed to Type 347 stainless steel side plates. The fuel plates are 0.060 in. thick. The fuel plate core is 0.050 in. thick and contains 25 w/o UO_2 (hydrothermal, Geneva, fully enriched, 270 to 100-mesh size) dispersed in Type 347 stainless steel. The core is clad with 0.005 in. of Type 347 stainless steel. The dimensions of the plates and subassembly are given in Figures 5 and 6.

The total uranium-235 content of the element used for the flux measurements is about 207 g. Table 1 lists the weights of the materials of the seven fuel plates in the element. The plate and UO_2 weights were determined by experimental measurements. The weights of the uranium-235 have been computed on the basis of the reported enrichment of the material.

TABLE 1. WEIGHTS OF CORE MATERIALS IN MARK I TEST ELEMENT

Fuel-Plate Position	Plate Weight, g	UO_2 Weight, g	Uranium Weight, g	Uranium-235 Weight, g
Top	145.45	36.36	31.74	29.56
2	144.43	36.11	31.52	29.35
3	146.67	36.67	32.01	29.81
4	148.50	37.13	32.41	29.84
5	146.53	36.63	31.97	29.77
6	146.32	36.58	31.93	29.74
Bottom	142.22	35.56	31.04	28.91
Total	1020.12	255.04	222.62	206.98

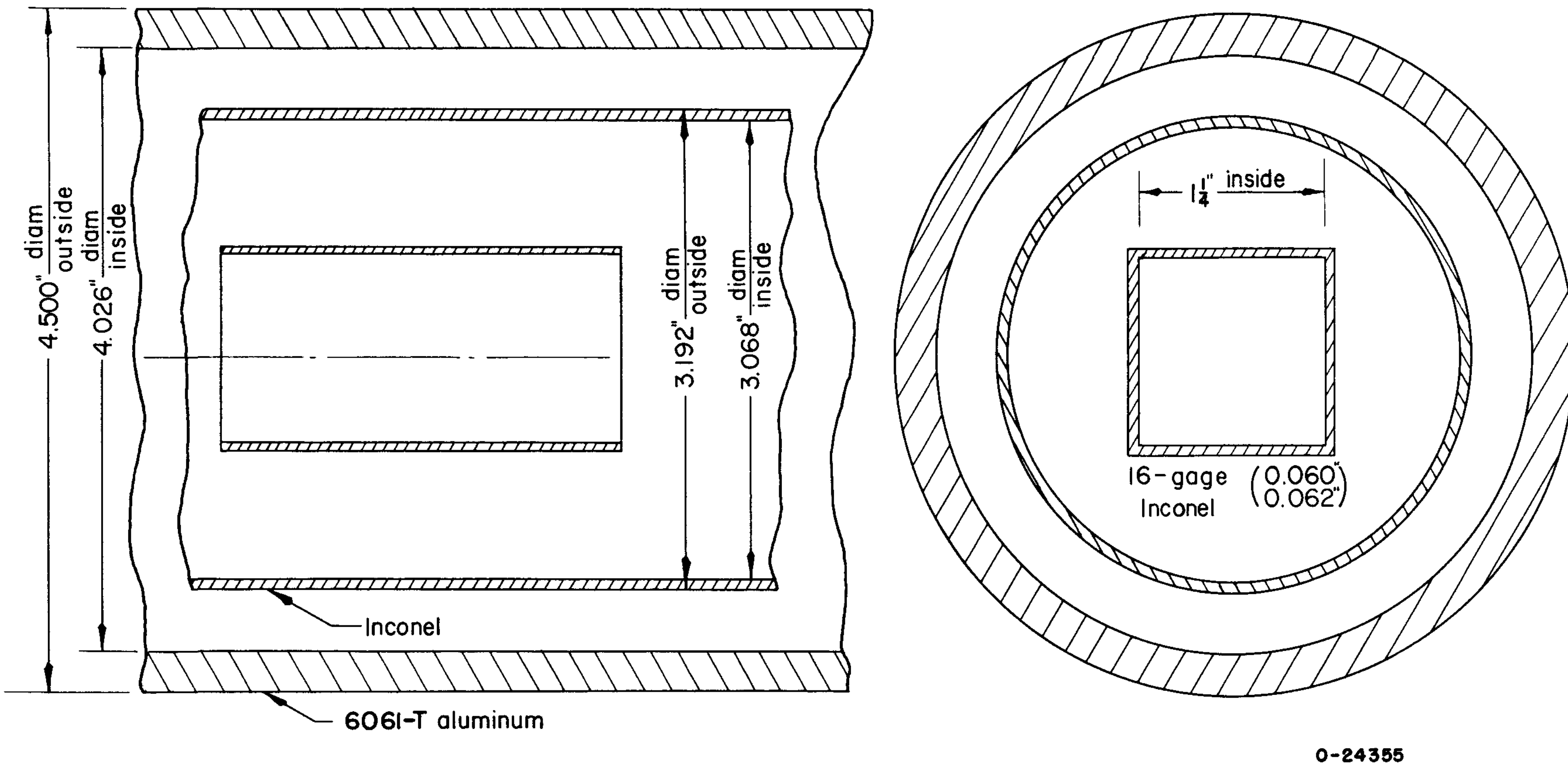

FIGURE 1. SKETCH OF LOOP CROSS SECTION

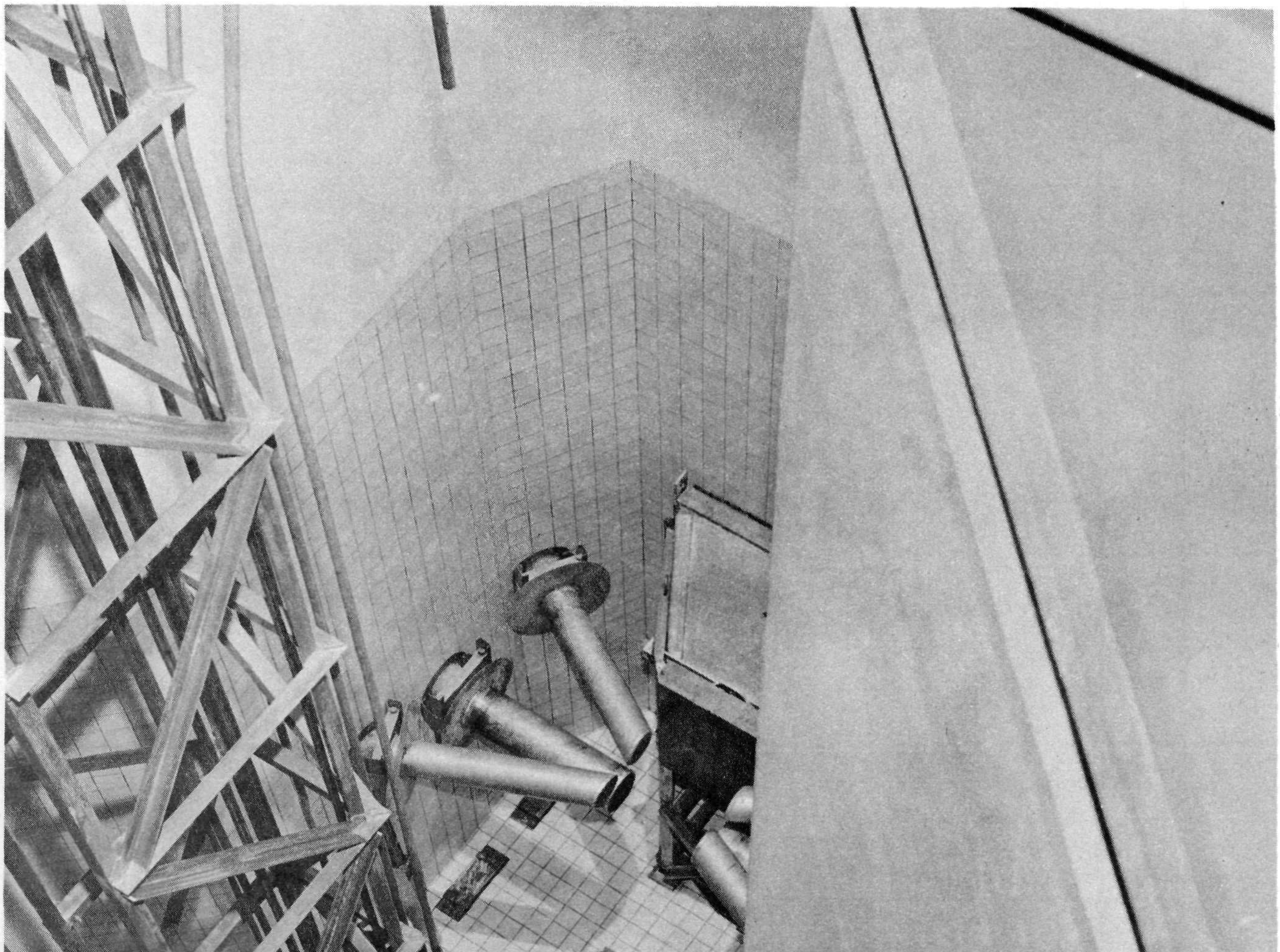

FIGURE 2. PHOTOGRAPH OF THE REACTOR TOWER AND INSTRUMENT TOWER

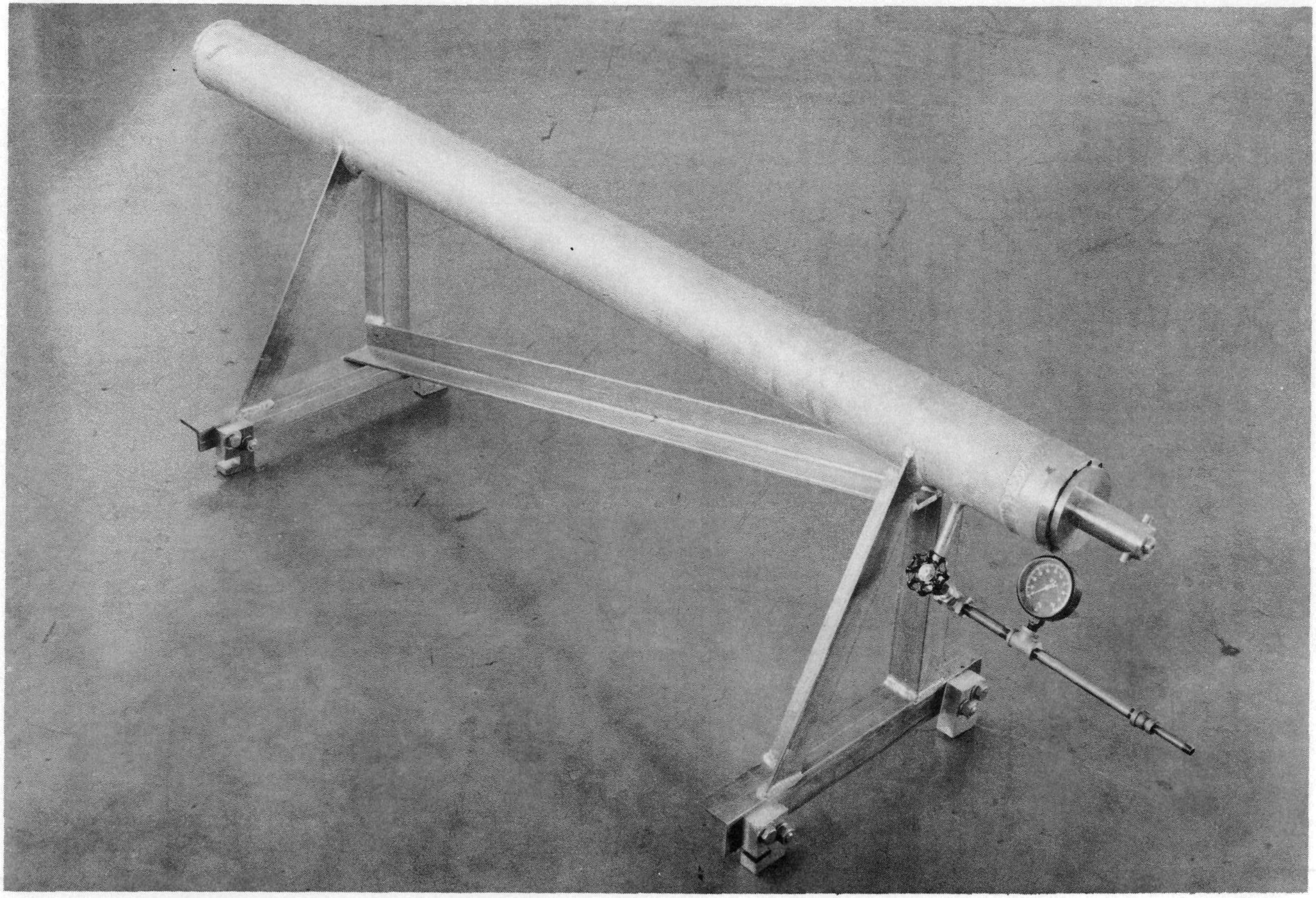

N41074

FIGURE 3. LOOP MOCK-UP AND SUPPORTING FRAME

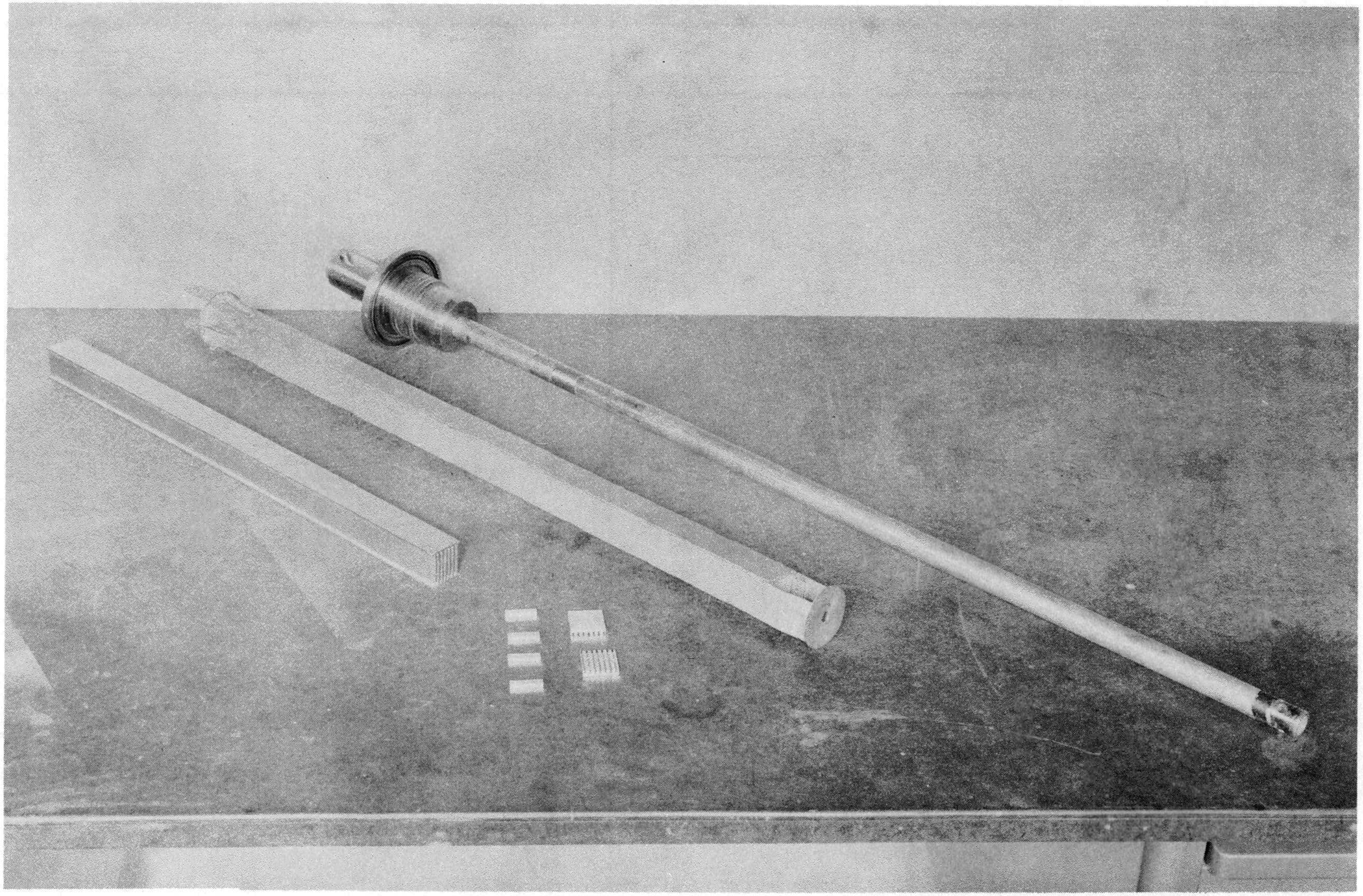

N41075

FIGURE 4. COMPONENTS OF CENTRAL PORTION OF LOOP

CONFIDENTIAL

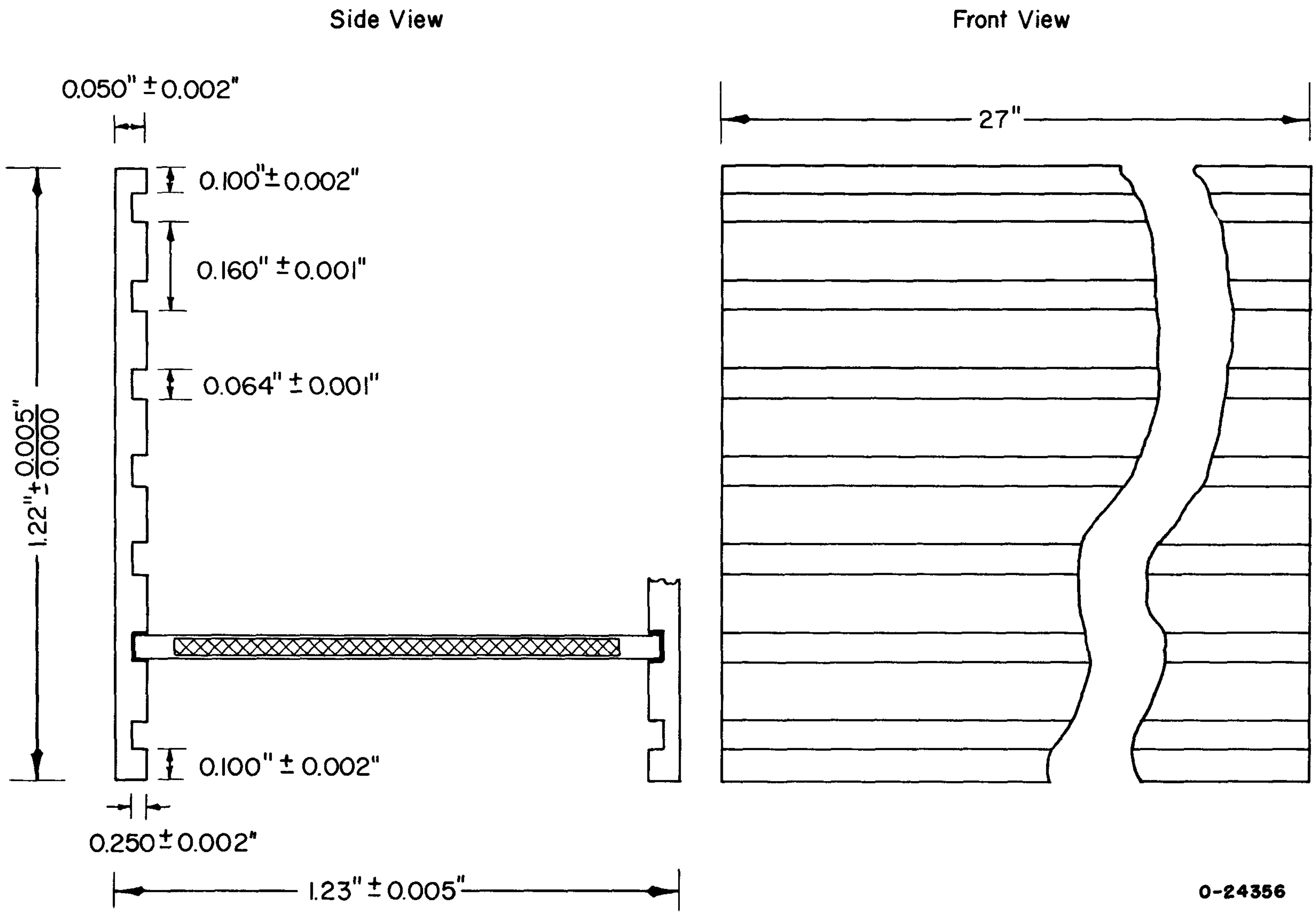

FIGURE 5. MARK I SUBASSEMBLY SIDE PLATES

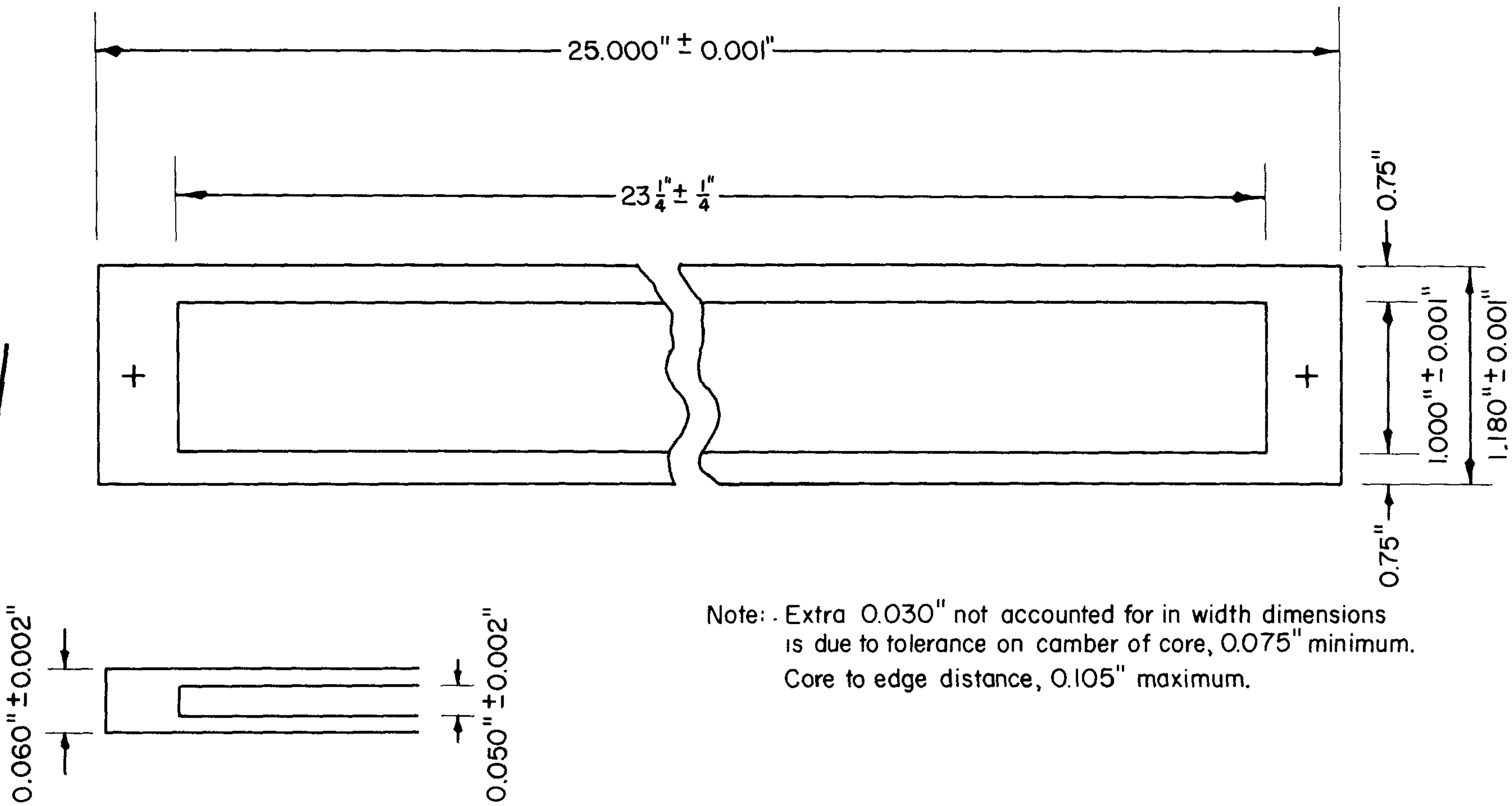

FIGURE 6. FUEL PLATE FOR THE MARK I ELEMENT

Wire Holders

The flux measurements were made in the test element by activating 0.033-in.-diameter manganese-iron wires which were positioned vertically in the channels adjacent to the fuel plates. In order to insure accurate and reproducible positioning of the wires, special aluminum end adapters were made for the test element to support the wires. These adapters can be seen in Figure 4 in front of the test element.

BATTELLE RESEARCH REACTOR CORE AND LOOP ARRANGEMENTS

The loop can be positioned in several locations near the face of the reactor core, and the core can be rearranged to allow addition of fuel elements in the neighborhood of the loop to form several convenient arrangements, depending on the magnitude of neutron flux desired. Flux measurements have been made with three combinations of loop position and core configuration. Measurements with these combinations will be designated as Series I, II, and III.

Series I measurements consisted of three runs with the reactor-core configuration shown in Figure 7. The initial run was made with the plates of the element parallel to the face of the BRR (orientation designated as zero deg), while the second run was a measurement of the flux distribution in the same position but with the fuel element removed. The third run of this series consisted of measurement of the cadmium ratio along the vertical center line of the element.

The Series II measurement was a zero-deg run with the reactor core loaded as shown in Figure 8.

For the measurements of Series III, both zero-deg and 90-deg orientations were studied with the reactor core loaded as shown in Figure 9. The Series III measurements were made after the original mounting of the loop was modified to shift the loop 1 in. along the face of the core toward the center.

EXPERIMENTAL PROCEDURES

Preparatory Experiments and Counting Techniques

To measure the flux, commercially available wires were irradiated and then suspended in the fuel element so as to contact the core side (front) of each fuel plate. Mounting plates were made to hold three wires on the front of each of the seven plates (see Figure 4).

Manganese-iron and aluminium-indium wires (.033-in. diameter) were irradiated, and the resulting radioactivity examined with a scintillation spectrometer. The gamma-energy spectrum of the manganese-iron wire was found to contain less distortion from

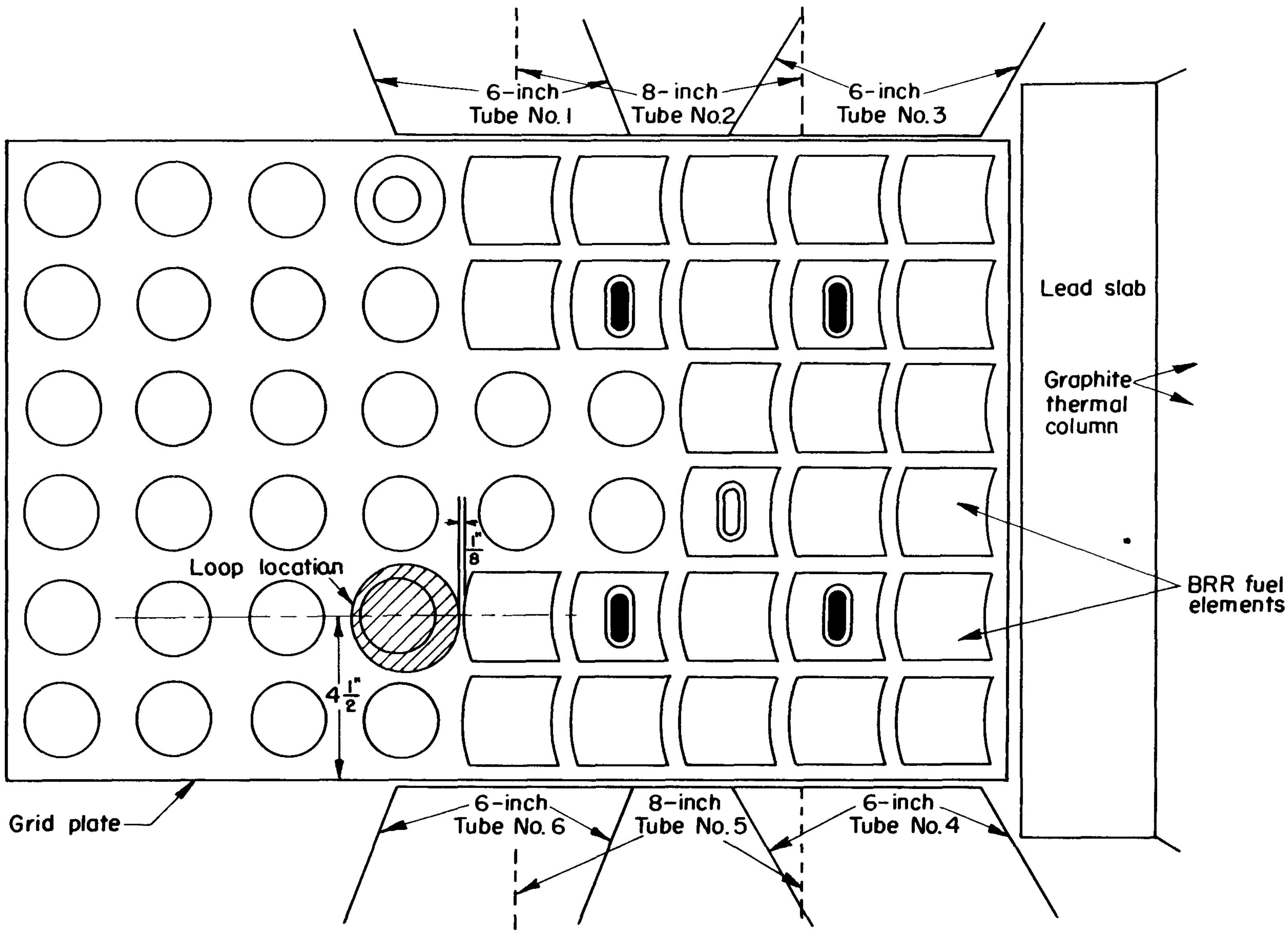

FIGURE 7. GENERAL ARRANGEMENT OF APB LOOP AND REACTOR CORE FOR SERIES I MEASUREMENTS

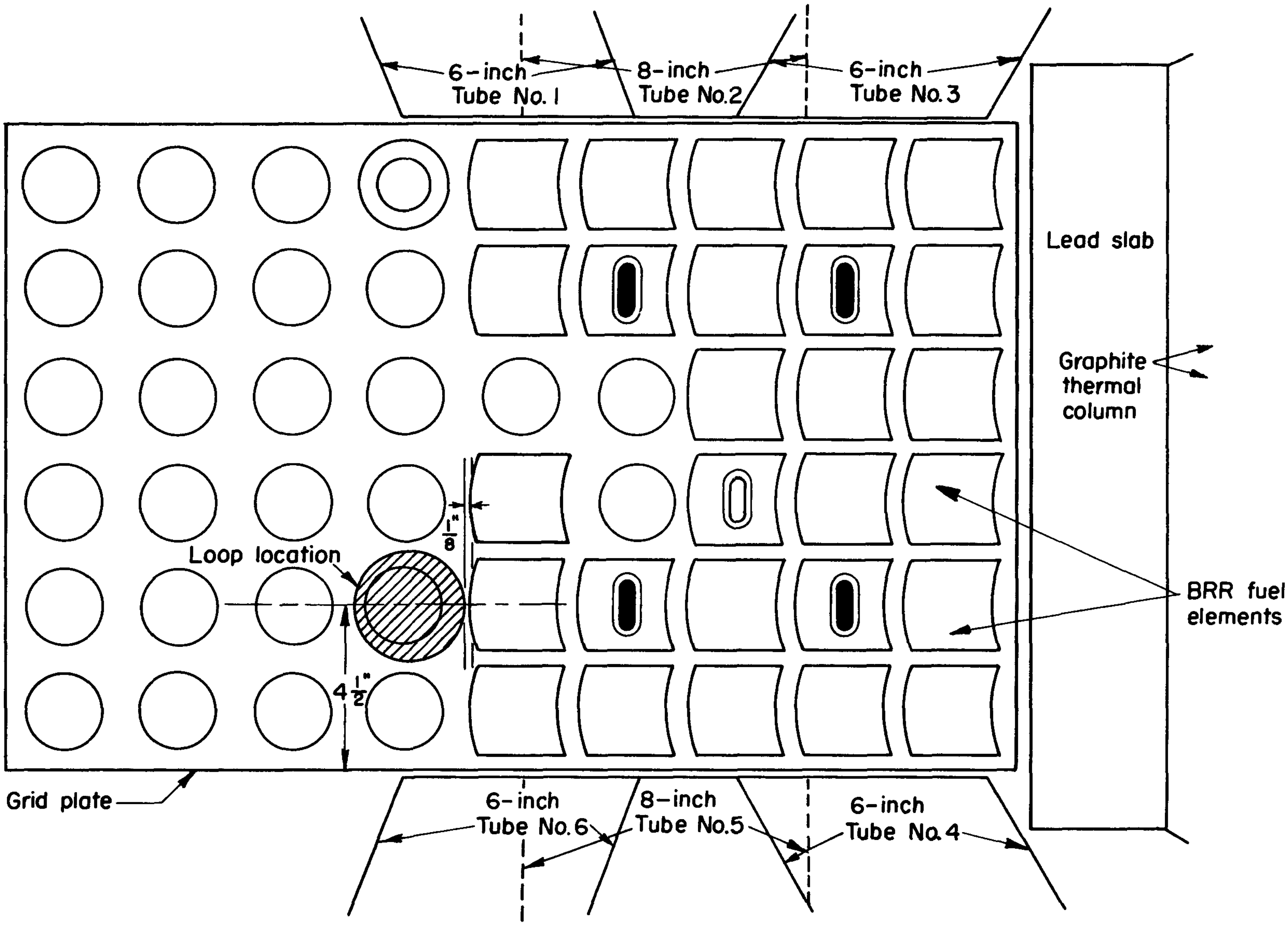

FIGURE 8. GENERAL ARRANGEMENT OF APB LOOP AND REACTOR CORE FOR SERIES II MEASUREMENTS

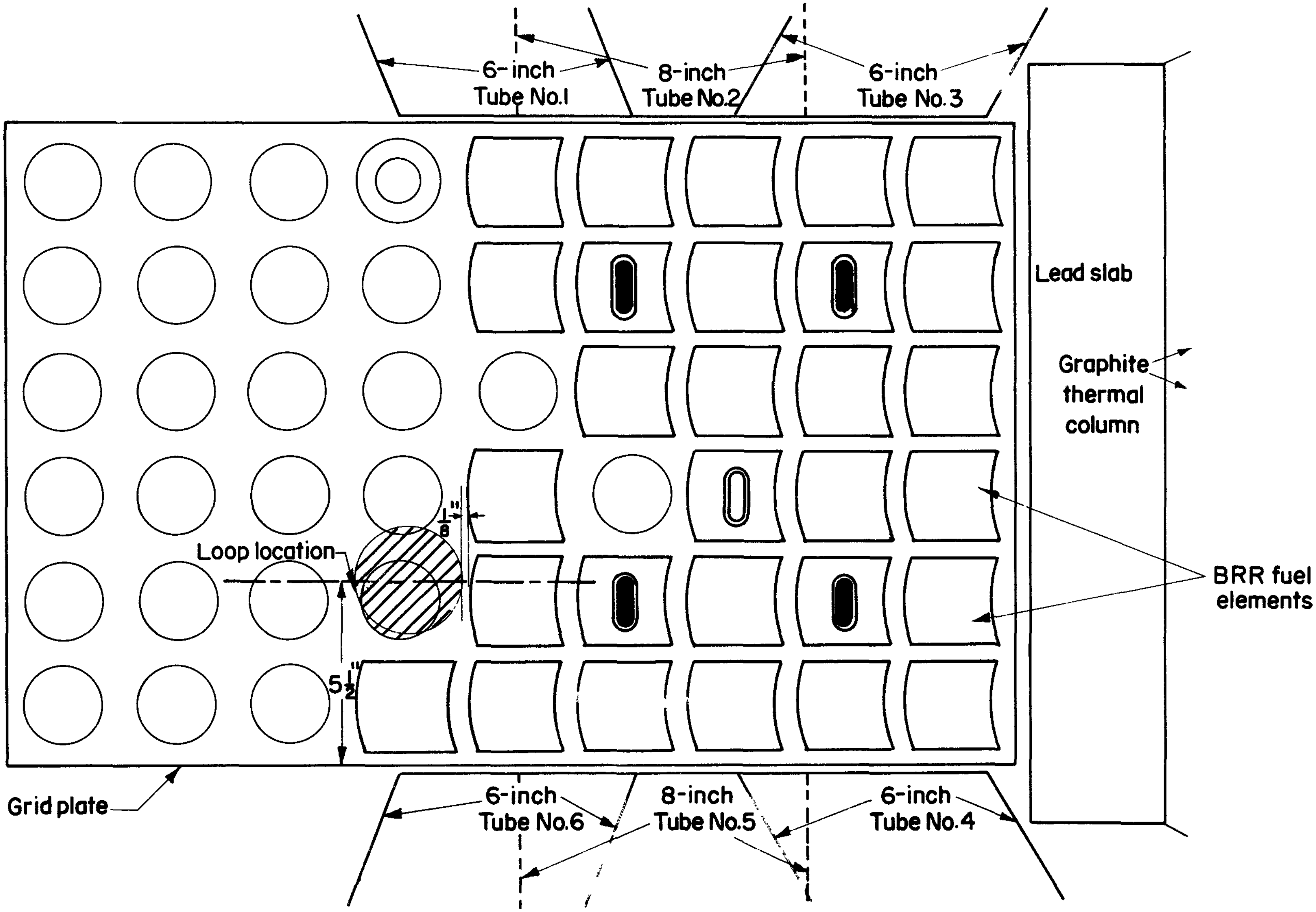

FIGURE 9. GENERAL ARRANGEMENT OF APB LOOP AND REACTOR CORE FOR SERIES III MEASUREMENTS

impurities in the wire and, hence, this wire was chosen for the flux measurements. Studies of the spectrum and half-life showed a clear 0.845-mev gamma peak corresponding to the manganese-56 radioisotope with the listed half-life of 2.58 hr*.

To assign absolute values to the induced activity of the wires, 0.001-in.-thick gold foils were positioned at selected locations in the fuel element along with the wires. Both uncovered and cadmium-covered foils were used. The foils were a 1/2-in.-diameter disk to match the geometry of a standard cesium-137 source. This source was standardized at the high-pressure gamma ionization chamber at ORNL to 0.875 microcuries ±3 per cent.

The thermal flux was then determined from the activity of the gold foil by using the relationship

$$\phi_{th} = \frac{A_o\left(1 - \frac{1}{R_{cd}}\right)}{\Sigma_a M\left(1-e^{-\lambda t_1}\right)\left(e^{-\lambda t_2}\right)E} ,$$

where

ϕ_{th} = thermal neutron flux, neutrons/(cm^2)/(sec)

A_o = activity of bare foil observed by scintillation counter, disintegrations/sec

R_{cd} = cadmium ratio = activity of bare foil/activity of cadmium-covered foil

Σ_a = macroscopic absorption cross section of gold, cm^2/g

M = mass of foil, g

λ = decay constant of gold, sec^{-1}

t_1 = length of exposure, sec

t_2 = time after exposure ended that A_o was observed, sec

E = efficiency of counter (see below).

Measurements of the induced activities of the wires and gold foils were made on a scintillation spectrometer composed of a manual sample changer equipped with a 1-3/4 by 2-in. Harshaw, sodium iodide, thallium-activated crystal and a DuMont Type 6929 photomultiplier tube. High voltage was supplied to the photomultiplier tube by an Atomic super-stable high-voltage supply, Model 312. Pulses from the photomultiplier were fed through an Atomic linear amplifier, Model 218, and an Atomic pulse-height analyser, Model 510, to a Berkeley digital counter.

The counter efficiency, E, used in the formula above is composed of the four factors E_c, E_w, E_s, and E_b:

E_c = geometrical and detection efficiency of the counter

E_w = counter-window absorption factor

*"Table of Isotopes", Hollander, J. M., Perlman, I., and Seaborg, G. T., University of California (December, 1952).

E_s = sample self-absorption factor

E_b = backscattering factor.

The ratio of the area under the photopeak to the area under the entire spectrum curve gives the photoefficiency of a crystal for a gamma ray of a particular energy. The gold foils were counted against the face of the crystal and were of the same size as the cesium standard to assure identical geometrical efficiency. Normalizing the photoefficiency of the gold to that of the cesium determines the E_c value. Counting under these circumstances reduces E_b to negligible proportions. In counting gamma rays, E_w and E_s may be neglected as very thin foils (0.001 in.), and counter windows are used. Counting was calibrated to the half-peak of the gold, with an over-all counter efficiency of approximately 1.8 per cent.

A complete spectrum analysis for cesium-137 and the activated gold-198 was taken just prior to counting each gold foil used for flux measurements to correct for temperature effects on counter efficiency.

Flux-Measuring Experiments

A jig was constructed to hold the test element so that the manganese-iron wires could be fed through the aluminum holders and secured with sufficient tension to keep them straight and in place against the fuel plates. A gold foil was centered in place on the front plate of the element and secured with nylon tape. After removing the test element from the jig and installing it in the loop, the loop was evacuated by a mechanical forepump for 24 hr and then filled to a pressure of 79.5 psi with nitrogen gas to simulate the nitrogen atmosphere which will be present at operating conditions in the reactor.

After positioning the loop on the instrument bridge, the bridge was rolled to within a few feet of the reactor bridge with the loop center line approximately 10 ft above the core. The reactor was brought to a critical state and the position of the safety rods noted. The reactor was then made subcritical. The loop was moved up to the core by first rolling the instrument bridge to a preset location and then lowering the loop until it rested on the element-locating grid pin (see Figure 10). The reactor was again made critical and the change in position of the safety rods at criticality was observed. From calibration curves of the safety rods the reactivity effect of the loop could be obtained.

The reactor was operated at a power of 500 w for 3 hr to activate the wires and foils for each experiment.

About 4 hr after shutdown, the loop was raised to the surface of the pool and the loop gas exhausted to a gas stack. The loop was then flushed with compressed air and the fuel element and holder were removed to extract the wires and foils. The wires were cut into 1-in. lengths and the activity of each length was counted. The induced activity of the wire sections was then normalized to the flux obtained from activation of the gold foil.

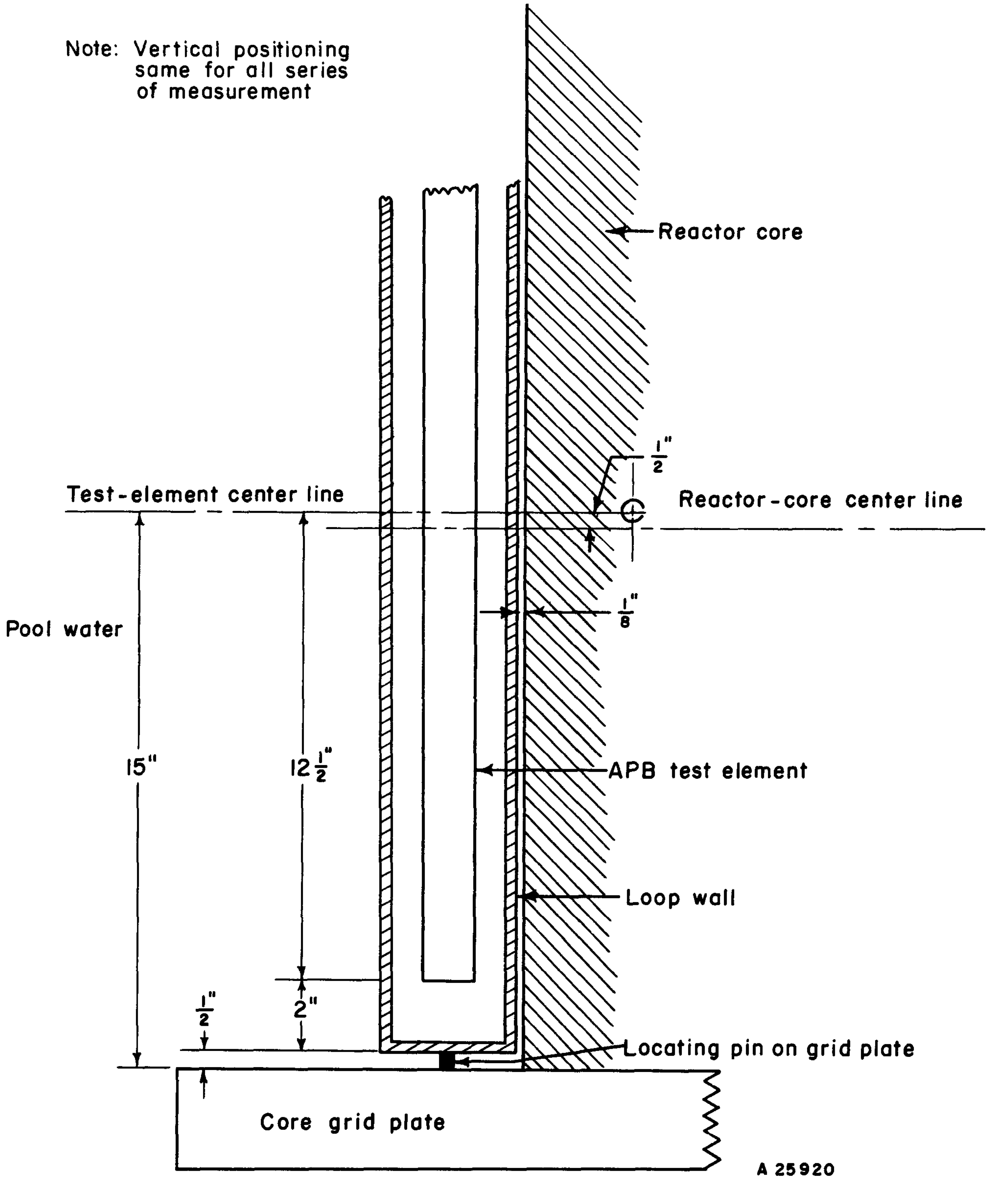

FIGURE 10. SKETCH OF VERTICAL LOCATION OF LOOP WITH RESPECT TO THE BRR CORE

RESULTS OF THE EXPERIMENTS

The wires were numbered in sequence as shown in Figure 11, and the 1-in. segments were designated as 1, 2, 3, etc., starting at the top of the element. This numbering system was used throughout the experiment and is used here to refer to physical positions. (For example, Wire 11, Position 13, is the 1-in. piece of the center wire, between 12 in. and 13 in. from the top of the element.)

The flux values obtained at low power were normalized to 1-megawatt reactor power level, which is the normal operating power of the BRR.

Series I Measurements

To reduce the measurements to thermal-neutron flux, a cadmium-covered wire was inserted in Position 11. The activity of the cadmium-covered wire was compared with the activity of a bare wire irradiated in the same location, and a cadmium ratio for each inch was computed. The results are given in Table 2. As a first approximation, it was assumed that the cadmium ratio in the element was constant in the horizontal plane. (A variation in the cadmium ratio of even 10 to 15 would amount to an error of less than 4 per cent thermal-neutron flux assigned to the wire activity.) The activity of the wire, corrected for the cadmium ratio, was then normalized to thermal-neutron flux by the gold-foil measurement.

The thermal-neutron flux was mapped in the loop with and without the test element. The flux values obtained are reported in Table 3. To present a picture of the flux variation in the horizontal plane, the flux values from Table 3 for the central cross section through the element are shown on the diagram in Figure 12. The gross flux variation in the vertical plane with the element in position can be seen from Figure 13, where the flux averaged over each horizontal cross section is plotted versus position of the cross section. The average thermal-neutron flux in the entire test element was found to be 0.564×10^{12} neutrons/(cm^2)(sec); hence, the power generation in the assembly for this particular core configuration (Series I) would be approximately 6 kw at 1-megawatt reactor power.

Figure 14 shows the gross flux variation in the vertical plane in the loop in the absence of the test element. The flux variation in the horizontal plane is shown in Figure 15 for the central cross section. The average thermal-neutron flux in the volume normally occupied by the test element was found to be 1.166×10^{12} neutrons/(cm^2)(sec). The thermal disadvantage factor for the system (defined as the ratio of the average thermal flux with the element in position to the average unperturbed thermal flux) is found from the above data to be 0.484.

Series II Measurements

As indicated earlier, the Series II measurements consisted of a zero-deg run with the reactor core modified as shown in Figure 8. The fluxes resulting from this change

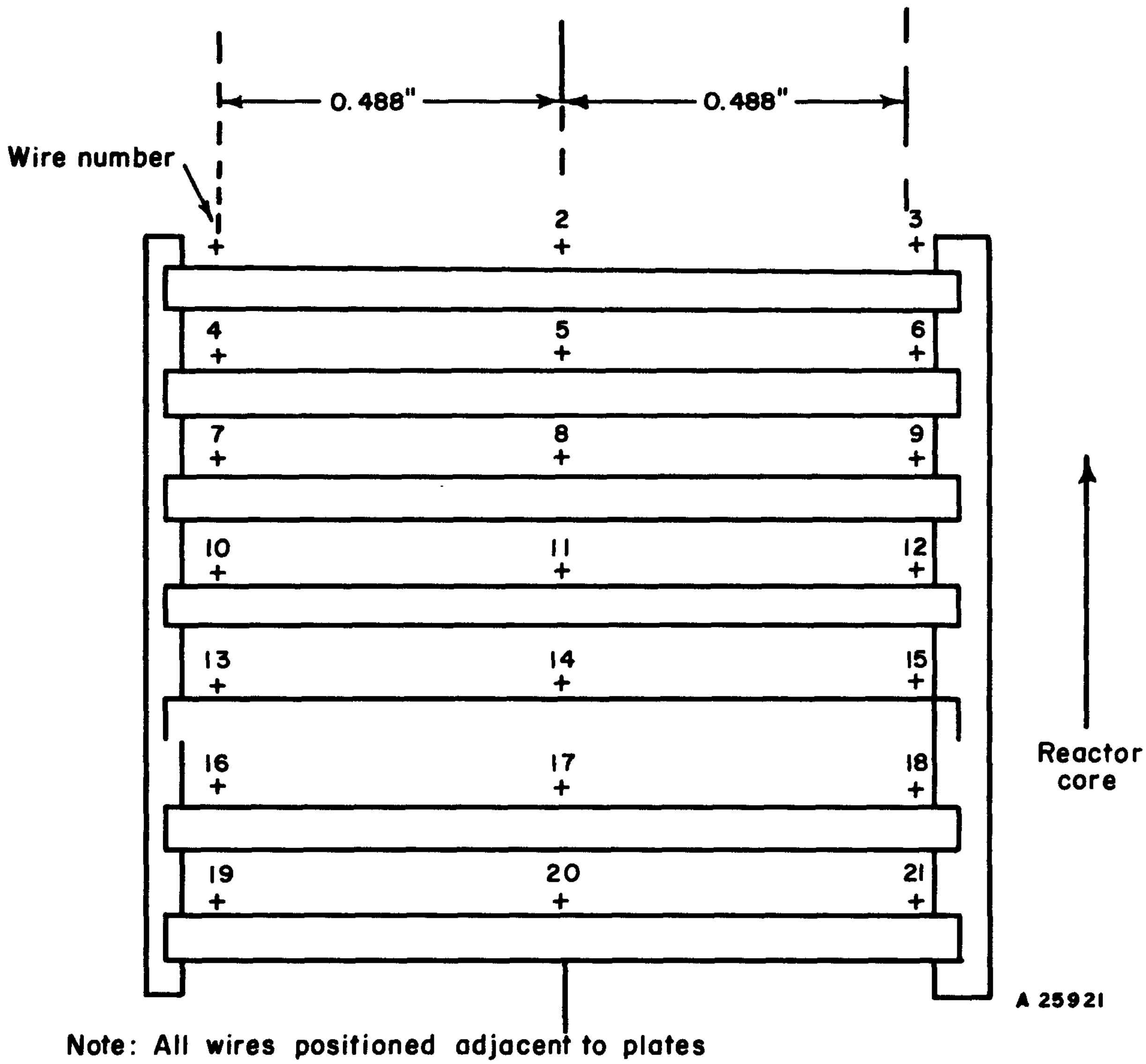

FIGURE 11. LOCATION AND NUMBERING SCHEME FOR MANGANESE-IRON WIRES

TABLE 2. CADMIUM RATIO ALONG VERTICAL CENTER LINE (POSITION 11) OF TEST ELEMENT

Cross-Section Number, N[a]	Cadmium Ratio
1	22.3
2	14.0
3	13.7
4	13.2
5	13.5
6	13.2
7	12.5
8	11.8
9	11.6
10	13.7
11	13.1
12	12.2
13	12.2
14	12.3
15	11.0
16	12.8
17	12.2
18	12.9
19	11.8
20	12.1
21	13.5
22	13.3
23	12.5
24	13.5
25	8.47

(a) The cross-section number, N, denotes that the cadmium ratios reported are the values measured for the range N-1 to N in. from the top of the element.

TABLE 3. THERMAL-NEUTRON-FLUX DATA FOR APB LOOP, SERIES I, WITH AND WITHOUT TEST ELEMENT

Cross Section Number, N(a)	Thermal-Neutron Flux, 10^{12} neutrons/(cm^2)(sec), for Indicated Wire Numbers (See Figure 11)					
	1		2		3	
	With	Without	With	Without	With	Without
1	0.440	0.396	0.437	0.573	0.362	0.468
2	0.450	0.592	0.413	0.618	0.392	0.538
3	0.507	0.716	0.451	0.716	0.471	0.661
4	0.550	0.710	0.534	0.822	--	0.730
5	0.647	0.899	0.685	0.991	0.583	0.833
6	0.684	0.952	0.748	1.063	0.679	0.836
7	0.735	0.975	0.810	1.141	0.803	0.902
8	0.805	0.979	0.893	1.171	0.873	1.135
9	0.941	0.951	0.951	1.197	0.932	1.225
10	1.048	0.908	1.029	1.214	1.066	1.261
11	1.063	0.845	1.035	1.220	1.220	1.395
12	1.074	0.872	1.047	1.184	1.111	1.441
13	1.120	0.850	1.083	1.138	1.230	1.432
14	1.149	0.823	1.130	1.167	1.231	1.553
15	1.209	0.760	1.145	1.145	1.264	1.400
16	1.254	0.807	1.162	1.226	1.282	1.438
17	1.285	0.771	1.083	1.193	1.276	1.432
18	1.282	0.867	1.088	1.217	1.484	1.484
19	1.244	0.869	1.071	1.254	1.144	1.418
20	1.183	0.917	0.972	1.284	1.100	1.357
21	1.130	0.963	0.907	1.250	1.028	1.370
22	1.027	1.027	1.809	1.240	0.925	1.193
23	0.948	1.086	1.676	1.122	0.837	1.187
24	0.824	1.065	0.596	1.037	0.764	1.019
25	0.632	0.944	0.637	0.900	--	--

TABLE 3. (Continued)

Cross Section Number, N(a)	Thermal-Neutron Flux, 10^{12} neutrons/(cm^2)(sec), for Indicated Wire Numbers (See Figure 11)					
	4		5		6	
	With	Without	With	Without	With	Without
1	0.280	0.451	0.259	--	0.390	0.503
2	0.265	0.607	0.214	--	0.336	0.581
3	0.302	0.627	0.252	--	0.378	0.627
4	0.360	0.776	0.318	--	0.424	0.752
5	0.407	0.945	0.352	--	0.463	0.811
6	0.478	0.906	0.424	--	0.517	0.933
7	0.541	1.003	0.505	--	0.547	1.067
8	0.619	1.162	0.565	--	0.623	1.180
9	0.668	1.197	0.578	--	0.652	1.243
10	0.750	1.261	0.617	--	0.775	1.326
11	0.799	1.432	0.647	--	0.742	1.423
12	0.837	1.331	0.684	--	0.657	1.469
13	0.946	1.487	0.658	--	0.691	1.487
14	0.832	1.553	0.709	--	0.730	1.544
15	0.909	1.527	0.664	--	0.791	1.518
16	0.908	1.512	0.715	--	0.829	1.614
17	0.881	1.533	0.675	--	0.812	1.561
18	0.882	1.503	0.650	--	0.798	1.567
19	0.833	1.427	0.618	--	0.855	1.464
20	0.798	1.385	0.624	--	0.799	1.440
21	0.718	1.315	0.597	--	0.898	1.269
22	0.659	1.221	0.537	--	0.768	1.203
23	0.538	1.086	0.488	--	0.689	1.086
24	0.601	0.991	0.432	--	0.659	1.019
25	0.572	0.820	0.468	--	0.572	0.878

TABLE 3. (Continued)

Cross Section Number, N(a)	Thermal-Neutron Flux, 10^{12} neutrons/(cm^2)(sec), for Indicated Wire Numbers (See Figure 11)					
	7		8		9	
	With	Without	With	Without	With	Without
1	0.368	--	0.261	--	0.308	0.481
2	0.298	--	0.185	--	0.290	0.557
3	0.319	--	0.202	--	0.294	0.649
4	0.360	--	0.243	--	0.318	0.784
5	0.425	--	0.265	--	0.332	0.854
6	0.441	--	0.318	--	0.360	0.952
7	0.477	--	0.338	--	0.388	1.021
8	0.502	--	0.385	--	0.424	--
9	0.519	--	0.406	--	0.406	1.234
10	0.561	--	0.408	--	0.433	1.233
11	0.582	--	0.436	--	0.457	1.368
12	0.591	--	0.470	--	0.466	1.359
13	0.642	--	0.561	--	0.512	1.405
14	0.646	--	0.512	--	0.526	1.480
15	0.672	--	0.553	--	0.577	1.500
16	0.698	--	0.531	--	0.498	1.429
17	0.678	--	--	--	0.529	1.423
18	0.644	--	0.544	--	0.569	1.429
19	0.573	--	0.519	--	0.573	1.409
20	0.591	--	0.470	--	0.557	1.330
21	0.575	--	0.454	--	0.530	1.296
22	0.546	--	0.382	--	0.515	0.934
23	0.496	--	0.387	--	0.512	0.876
24	0.487	--	0.374	--	0.430	0.778
25	0.467	--	0.387	--	0.577	0.669

TABLE 3. (Continued)

Cross Section Number, N(a)	Thermal-Neutron Flux, 10^{12} neutrons/(cm^2)(sec), for Indicated Wire Numbers (See Figure 11)					
	10		11		12	
	With	Without	With	Without	With	Without
1	0.289	0.516	0.290	--	0.290	0.471
2	0.238	0.573	0.206	--	0.286	0.574
3	0.248	0.665	0.239	--	0.307	0.679
4	0.276	0.705	0.274	--	0.339	0.789
5	0.277	0.886	0.310	--	0.386	0.895
6	--	0.906	0.334	--	0.453	0.998
7	0.422	1.076	0.354	--	0.510	1.067
8	0.448	1.098	0.411	--	0.523	1.208
9	0.487	1.243	0.409	--	0.572	1.225
10	0.525	1.279	0.476	--	0.561	1.363
11	0.575	1.358	0.473	--	0.638	1.395
12	0.600	1.322	0.436	--	0.735	1.441
13	0.609	1.432	0.438	--	0.783	1.432
14	0.646	1.489	0.450	--	0.717	1.443
15	0.651	1.454	0.416	--	0.746	1.554
16	0.673	1.549	0.465	--	0.691	1.577
17	0.647	1.460	0.442	--	0.712	1.579
18	0.611	1.411	0.431	--	0.724	1.604
19	0.601	1.437	0.373	--	0.693	1.418
20	0.624	1.330	0.387	--	0.615	1.385
21	0.571	1.315	0.382	--	0.571	1.324
22	0.532	1.295	0.349	--	0.592	1.277
23	0.517	1.141	0.328	--	0.584	1.141
24	0.483	1.037	0.294	--	0.559	1.093
25	0.481	0.917	0.364	--	0.596	0.961

TABLE 3. (Continued)

Cross Section Number, N[(a)]	Thermal-Neutron Flux, 10^{12} neutrons/(cm^2)(sec), for Indicated Wire Numbers (See Figure 11)					
	13		14		15	
	With	Without	With	Without	With	Without
1	0.333	0.476	0.251	--	0.472	--
2	0.282	0.603	0.177	--	0.290	--
3	0.302	0.663	0.164	--	0.340	--
4	0.347	0.798	0.230	--	0.394	--
5	0.378	0.912	0.269	--	0.449	--
6	0.436	0.989	0.273	--	0.511	--
7	0.464	1.030	0.305	--	0.568	--
8	0.523	1.308	0.327	--	0.590	--
9	0.506	1.280	0.346	--	0.574	--
10	0.544	1.381	0.387	--	0.563	--
11	0.557	1.377	0.528	--	0.581	--
12	0.545	1.423	0.391	--	0.662	--
13	0.621	1.487	0.417	--	0.691	--
14	0.626	1.562	0.425	--	0.726	--
15	0.647	1.627	0.421	--	0.690	--
16	0.632	1.531	0.452	--	0.732	--
17	0.612	1.533	0.433	--	0.725	--
18	0.598	1.567	0.427	--	0.715	--
19	0.576	1.510	0.382	--	0.705	--
20	0.561	1.394	0.391	--	--	--
21	0.543	1.343	0.404	--	0.664	--
22	0.449	1.208	0.349	--	0.542	--
23	0.418	1.205	0.317	--	0.510	--
24	0.374	1.074	0.303	--	0.540	--
25	0.392	0.882	0.380	--	0.536	--

TABLE 3. (Continued)

Cross Section Number, N[a]	Thermal-Neutron Flux, 10^{12} neutrons/(cm^2)(sec), for Indicated Wire Numbers (See Figure 11)					
	16		17		18	
	With	Without	With	Without	With	Without
1	0.308	0.514	0.277	0.611	0.295	0.451
2	0.240	0.607	0.194	0.605	0.279	0.561
3	0.273	0.784	0.260	0.679	0.286	0.770
4	0.289	0.961	0.269	0.780	0.365	0.800
5	0.344	1.04	0.316	0.926	0.412	1.07
6	0.394	1.183	0.360	0.961	0.481	1.044
7	--	1.168	0.397	1.168	0.510	1.113
8	0.589	1.382	0.406	1.153	0.535	1.162
9	0.664	1.398	0.448	1.325	0.585	1.289
10	0.694	1.483	0.429	1.455	0.622	1.465
11	0.712	1.478	0.432	1.478	0.620	1.423
12	0.663	1.570	0.437	1.607	0.675	1.561
13	0.712	1.570	0.465	1.524	0.633	1.662
14	0.680	1.608	0.463	1.617	0.696	1.617
15	0.651	1.573	0.458	1.609	0.668	1.618
16	0.573	1.558	0.460	1.614	0.644	1.641
17	0.600	1.625	0.442	1.607	0.611	1.616
18	0.534	1.669	0.468	1.540	0.644	1.595
19	0.515	1.510	0.427	1.427	0.598	1.537
20	0.462	1.403	0.433	1.467	0.487	1.495
21	0.432	1.389	0.397	1.408	0.483	1.435
22	0.386	1.258	0.344	1.267	0.475	1.323
23	0.367	1.224	0.326	1.196	0.497	1.214
24	0.370	1.139	0.317	1.167	0.385	1.139
25	0.415	0.829	0.491	0.953	0.540	0.882

TABLE 3. (Continued)

Cross Section Number, N[(a)]	Thermal-Neutron Flux, 10^{12} neutrons/(cm^2)(sec), for Indicated Wire Numbers (See Figure 11)					
	19		20		21	
	With	Without	With	Without	With	Without
1	0.321	0.516	0.265	0.568	--	0.361
2	0.320	0.581	0.209	0.554	--	0.594
3	0.362	0.665	0.215	0.635	--	0.679
4	0.457	0.767	0.307	0.729	--	0.806
5	0.483	0.757	0.307	0.846	--	0.913
6	0.616	0.897	0.378	0.989	--	0.989
7	0.617	1.113	0.443	1.067	--	1.224
8	0.646	1.199	0.412	1.089	--	1.208
9	0.735	1.307	0.485	1.289	--	1.362
10	0.766	1.391	0.563	1.233	--	1.437
11	0.775	1.478	0.512	1.386	--	1.432
12	0.871	1.607	0.517	1.487	--	1.726
13	0.838	1.662	0.566	1.744	--	1.873
14	0.896	1.452	0.550	1.498	--	1.617
15	0.866	1.427	0.527	1.636	--	1.518
16	0.861	1.484	0.535	1.586	--	--
17	0.825	1.570	0.533	1.515	--	--
18	0.798	1.457	0.523	1.531	--	--
19	0.788	1.373	0.486	1.455	--	--
20	0.693	1.632	0.479	1.431	--	--
21	0.685	1.306	0.454	1.333	--	--
22	0.671	1.249	0.336	--	--	--
23	0.567	1.104	0.372	--	--	--
24	0.589	0.963	0.353	--	--	--
25	0.512	0.882	0.416	--	--	--

(a) The cross section number, N, denotes that the fluxes reported are the values measured for the range N-1 to N in. from the top of the element.

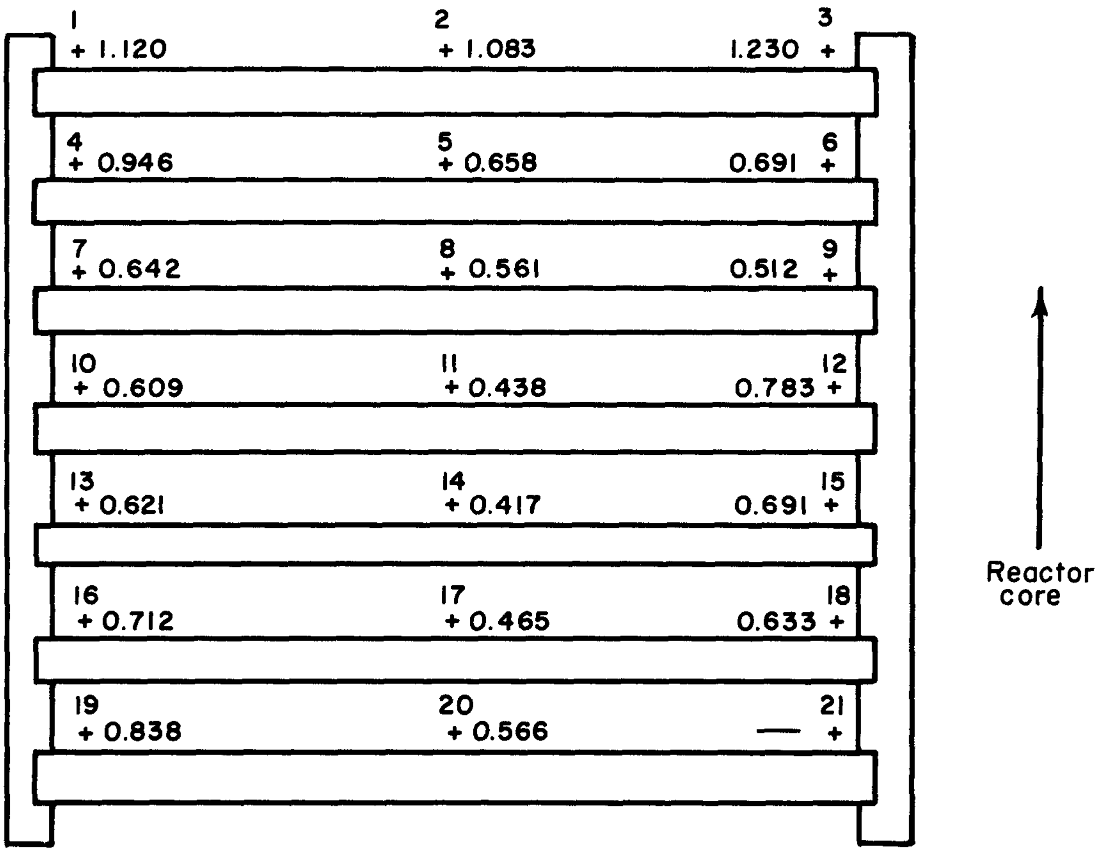

Cross-section number N,=13(denotes that the fluxes reported are the values measured for the range N-1 to N in. from the top of the element).

A 25922

FIGURE 12. HORIZONTAL CROSS-SECTIONAL TABULATION OF SERIES I FLUX MEASUREMENTS FOR APB TEST ELEMENT

Flux values are given in terms of 10^{12} neutrons/ (cm^2) (sec).

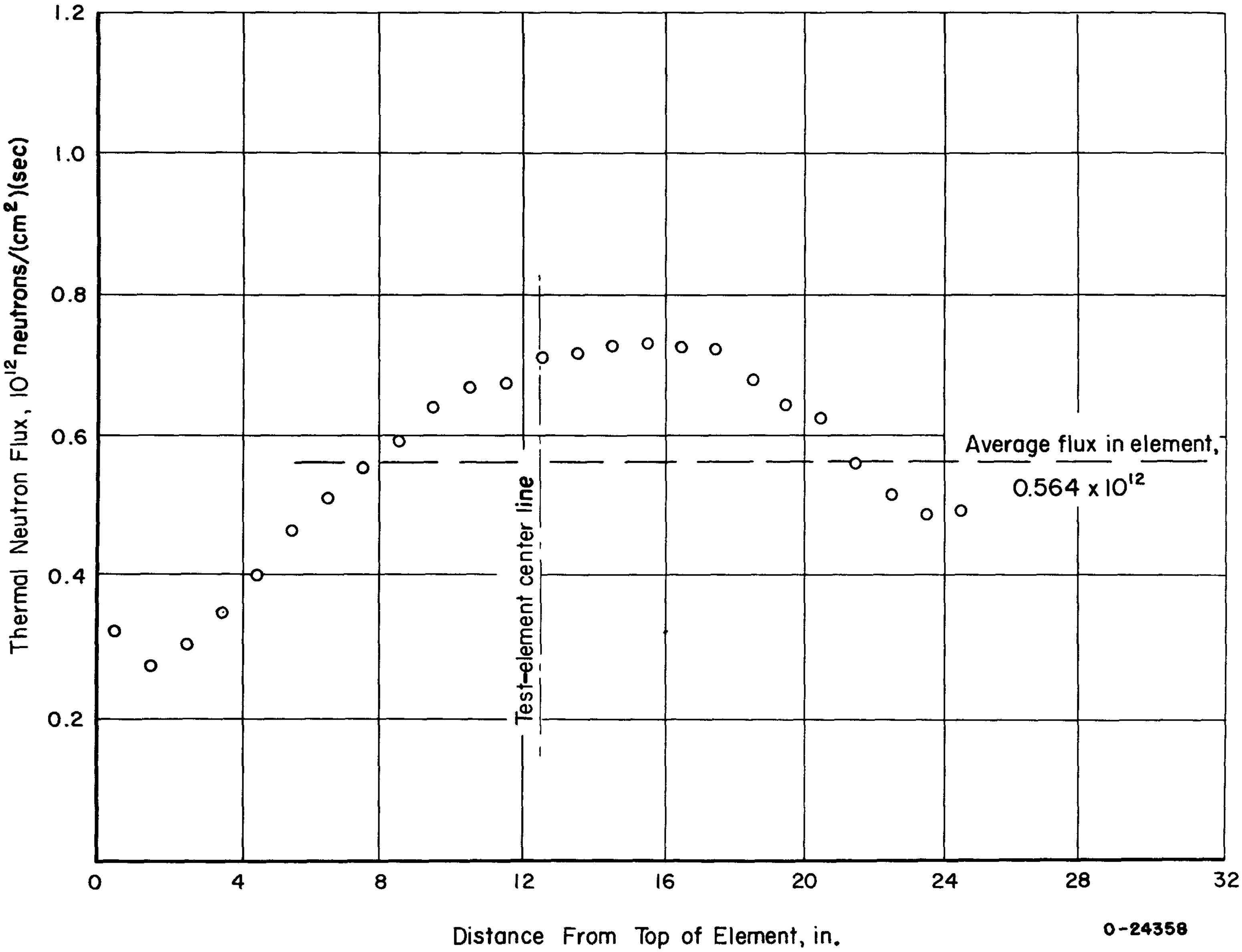

FIGURE 13. AVERAGE THERMAL-NEUTRON FLUX OVER EACH HORIZONTAL CROSS SECTION VERSUS LOCATION IN ELEMENT, SERIES I

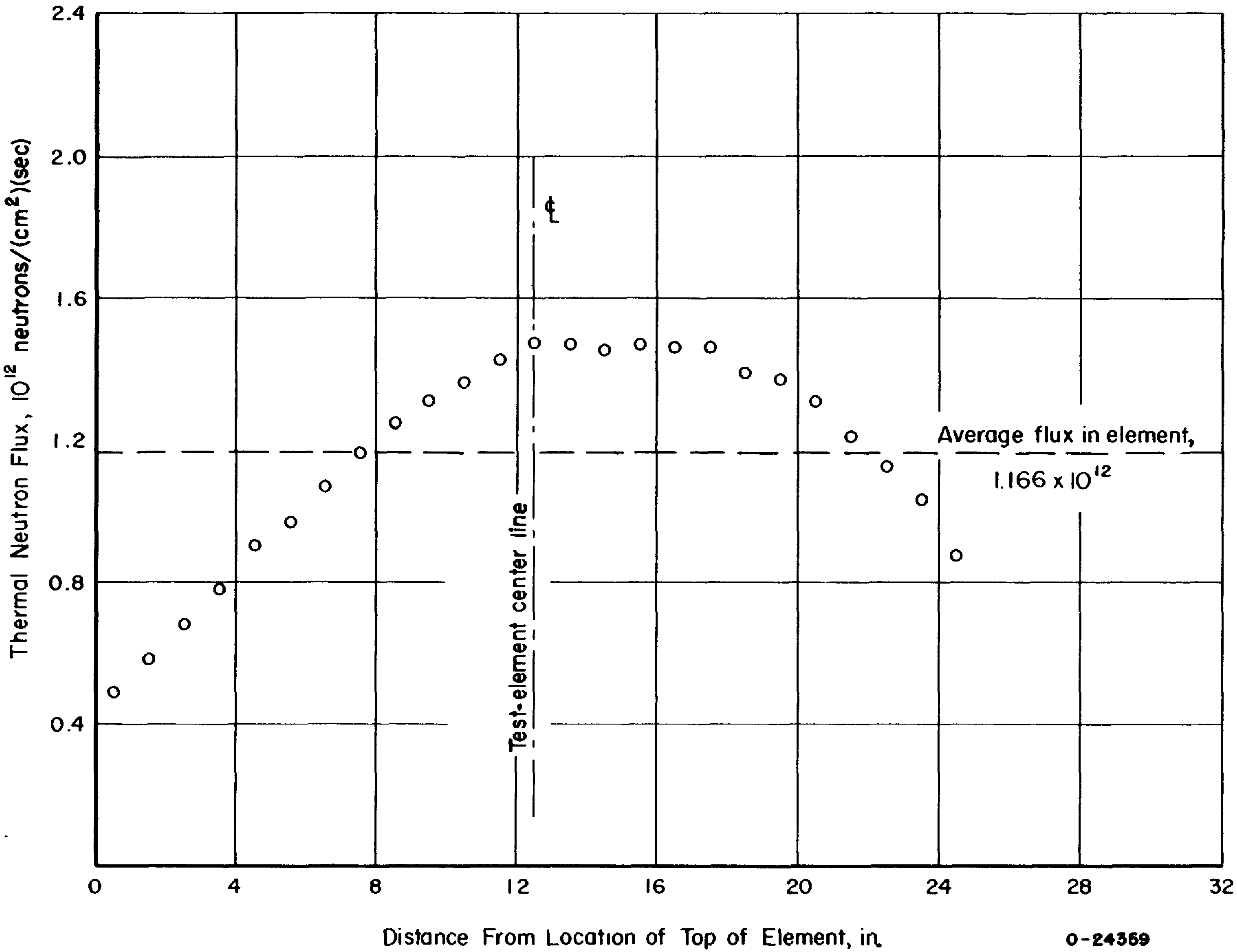

FIGURE 14. AVERAGE THERMAL-NEUTRON FLUX OVER EACH HORIZONTAL CROSS SECTION VERSUS LOCATION IN LOOP WITHOUT TEST ELEMENT, SERIES I

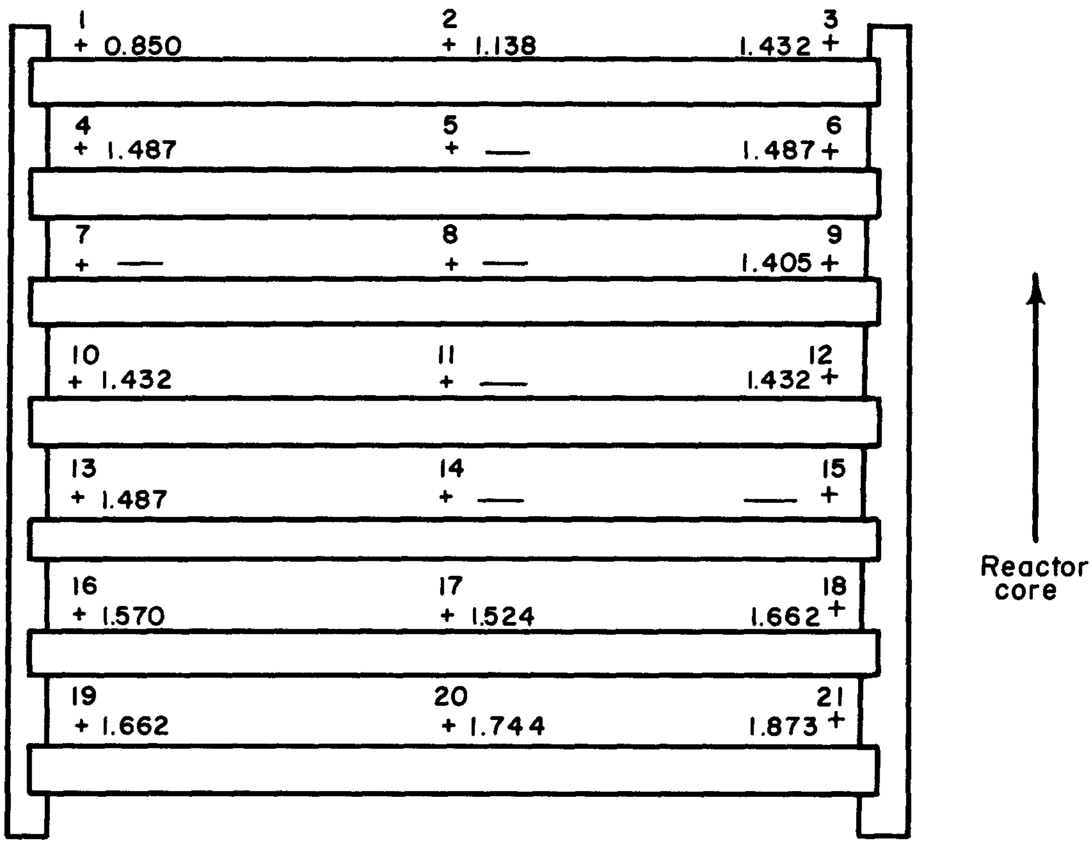

Cross-section number, N,=13(denotes that the fluxes reported are the values measured for the range N-1 to N in. from the top of the element).

A 25923

FIGURE 15. HORIZONTAL CROSS-SECTIONAL TABULATION OF SERIES I FLUX MEASUREMENTS FOR APB LOOP WITHOUT TEST ELEMENT

Flux values are given in terms of 10^{12} neutrons/ (cm^2) (sec).

are given in Table 4. The gross flux variation in the vertical direction is shown in Figure 16. With the average thermal-neutron flux of 2.24 x 10^{12} neutrons/(cm^2)(sec), the power generation in the assembly would be approximately 25 kw at 1-megawatt reactor power.

Series III Measurements

The third loop and core arrangement (shown in Figure 9) resulted in a further increase in the neutron flux in the loop. The values of the flux are tabulated in Table 5. To present a picture of the flux variation in the horizontal plane, the flux values from Table 5 for three horizontal cross sections through the element are shown in Figures 17, 18, and 19. As seen from these diagrams, the thermal flux depression from the edge of the element to the center is less than a factor of two. The gross flux variations in the axial direction for this run are shown graphically in Figure 20. The average thermal-neutron flux for the entire test element was found to be 4.90 x 10^{12} neutrons/(cm^2)(sec), producing a power of approximately 45 kw. The power generation can be decreased, of course, by backing the loop away from the core face into a lower flux region. The ratio of peak thermal flux (the maximum flux value measured in the element) to average thermal flux in the element was found to be 1.87.

The test element was then rotated 90 deg in the loop and the flux again mapped. The resulting neutron fluxes are given in Table 6. The average flux measured in the element at 90-deg rotation was found to be 3.91 x 10^{12} neutrons/(cm^2)(sec) compared with 4.09 x 10^{12} average flux at zero deg. Although the rotation of the element changed the flux distribution slightly, the average flux remained about the same.

An attempt to measure the "fine structure" of the flux distribution was made at the conclusion of the Series III measurements. The horizontal flux variation across the channel width was measured by gold foils. These foils were 1.0 mil by approximately 1.13 in. by 0.50 in. and were placed on the front and rear surface of the element as indicated in Figure 1. After irradiation, the foils were cut into segments approximately 0.05 in. wide. The width was established by weighing each segment and then multiplying this weight by a constant determined by multiple weighings of a known width of the foil. No attempt was made to correct the activity of the foil segments for any variation of the ratio of thermal to resonance flux ratio across the face of the plates. Table 7 gives the specific activity of these foils. Foil numbers refer to positioning as indicated on Figure 21. The activity of the segments of Foil 5 is shown graphically in Figure 22.

REACTIVITY EFFECT OF THE LOOP ON BRR CORE

The change in reactivity caused by the gas-filled loop and the fuel element in place at the face of the reactor core was less than the experimental accuracy of the measurements. The minimum reactivity change which can be measured with the present equipment is about 0.0005 $\frac{\Delta k_{eff}}{k_{eff}}$. This result is interpreted as indicating that

TABLE 4. THERMAL-NEUTRON-FLUX DATA FOR APB LOOP, SERIES II

Cross Section Number, N(a)	Thermal-Neutron Flux, 10^{12} neutrons/(cm^2)(sec), for Indicated Wire Numbers (See Figure 11)						
	1	2	3	4	5	6	7
1	2.14	1.76	1.92	1.83	1.30	1.61	1.42
2	1.76	1.67	1.83	1.46	1.12	1.43	1.26
3	1.85	1.86	2.10	1.74	1.29	1.81	1.39
4	2.35	2.10	2.38	1.94	1.41	1.85	1.58
5	2.68	2.42	2.83	2.27	1.56	2.10	1.80
6	3.00	2.67	3.10	2.52	1.82	2.20	1.95
7	3.31	2.96	3.47	2.79	1.92	2.39	2.20
8	3.56	3.15	3.89	2.89	2.03	2.43	2.26
9	3.71	3.24	3.94	3.05	2.11	2.71	2.00
10	4.08	3.51	4.27	3.15	2.34	2.82	2.52
11	4.17	3.73	4.31	3.36	2.33	2.81	2.62
12	4.18	3.84	4.28	3.23	2.45	2.96	2.73
13	4.23	3.91	4.54	3.26	2.48	2.99	1.87
14	4.35	4.00	4.17	3.33	2.49	3.01	2.89
15	4.31	3.76	4.16	3.28	2.46	2.91	2.90
16	4.21	3.89	4.14	3.18	2.48	2.90	2.73
17	4.10	3.79	3.86	3.15	2.34	2.74	2.74
18	3.95	3.50	3.83	3.01	2.33	2.62	2.59
19	3.70	3.35	3.57	2.83	2.15	2.46	2.38
20	3.72	3.05	3.39	2.58	2.01	2.30	2.28
21	3.45	2.86	4.50	2.40	1.83	2.08	2.01
22	3.03	2.69	2.76	2.19	1.64	2.03	1.88
23	2.70	2.37	2.50	1.95	1.45	1.95	1.77
24	--	2.31	2.41	2.05	1.91	2.29	1.92

TABLE 4. (Continued)

Cross Section Number, N[(a)]	Thermal-Neutron Flux, 10^{12} neutrons/(cm^2)(sec), for Indicated Wire Numbers (See Figure 11)						
	8	9	10	11	12	13	14
1	1.33	1.30	1.33	--	1.63	1.73	0.712
2	0.86	1.16	1.23	1.51	1.48	1.55	0.796
3	0.90	1.42	1.44	1.56	1.61	1.59	0.829
4	1.11	1.57	1.61	1.13	1.64	1.61	0.823
5	1.14	1.77	1.74	1.43	1.75	1.77	1.06
6	1.40	1.97	1.98	1.37	2.03	1.85	1.24
7	1.45	2.14	2.08	1.64	2.55	2.47	1.19
8	1.51	2.19	2.28	1.85	1.89	--	1.25
9	1.58	2.40	2.33	2.01	2.79	2.52	1.38
10	1.70	2.60	2.70	2.22	2.75	2.25	1.51
11	1.81	2.82	2.76	4.58	3.02	2.87	1.51
12	1.78	2.83	2.91	2.25	2.39	--	1.50
13	1.78	3.23	2.64	2.23	2.48	2.49	1.51
14	1.76	2.99	2.74	2.19	2.52	2.50	1.60
15	1.74	2.65	2.42	1.86	2.69	2.58	1.63
16	1.78	2.33	2.77	1.74	2.52	2.46	1.66
17	1.15	2.16	2.78	1.60	2.21	2.47	2.17
18	1.65	2.00	2.22	1.78	2.25	--	1.43
19	1.59	1.98	2.00	1.58	2.41	--	--
20	1.58	1.78	1.89	1.71	2.24	2.02	1.28
21	1.42	1.63	1.95	1.50	2.06	2.13	1.04
22	1.38	1.67	1.65	1.24	1.78	1.84	1.20
23	1.11	1.45	1.39	1.10	1.69	1.72	0.758
24	1.50	1.66	1.57	1.50	1.97	2.00	0.994

TABLE 4. (Continued)

Cross Section Number, N[a]	Thermal-Neutron Flux, 10^{12} neutrons/(cm^2)(sec), for Indicated Wire Numbers (See Figure 11)						
	15	16	17	18	19	20	21
1	1.31	1.27	1.04	2.12	1.35	1.16	1.39
2	0.97	1.28	0.708	1.29	1.26	0.95	1.33
3	1.43	1.41	0.776	1.44	1.41	1.18	1.19
4	1.53	1.44	0.95	1.70	1.71	1.03	1.62
5	1.75	1.81	1.21	1.90	1.92	1.25	1.90
6	2.08	2.08	1.33	2.15	2.14	1.47	2.06
7	2.19	2.43	1.60	2.12	2.39	1.58	2.16
8	2.36	2.32	1.18	2.21	2.50	1.76	2.19
9	2.24	2.49	1.51	2.49	2.65	1.58	2.51
10	2.49	2.76	1.67	2.75	2.77	2.06	2.36
11	2.56	2.75	1.77	2.81	2.87	1.72	2.72
12	2.93	2.60	1.51	3.33	--	2.13	2.89
13	2.64	2.65	1.77	2.81	2.36	2.52	3.35
14	--	2.77	1.91	2.68	3.02	2.16	3.38
15	2.61	2.67	1.71	2.77	2.78	--	2.84
16	2.65	2.68	1.96	2.95	2.65	2.17	2.91
17	2.92	2.52	1.74	2.75	2.48	2.17	2.68
18	2.54	2.45	1.66	2.53	2.50	2.20	2.59
19	2.36	2.31	1.79	2.36	2.31	1.83	2.46
20	2.19	1.81	1.38	2.18	2.25	1.69	2.29
21	1.98	2.03	1.31	1.97	2.04	1.63	2.29
22	1.79	1.75	1.28	1.79	1.79	1.12	1.90
23	1.74	1.63	1.19	1.59	1.79	1.15	1.72
24	1.89	2.02	1.37	1.85	1.62	1.37	1.81

(a) The cross section number, N, denotes that the fluxes reported are the values measured for the range N-1 to N in. from the top of the element.

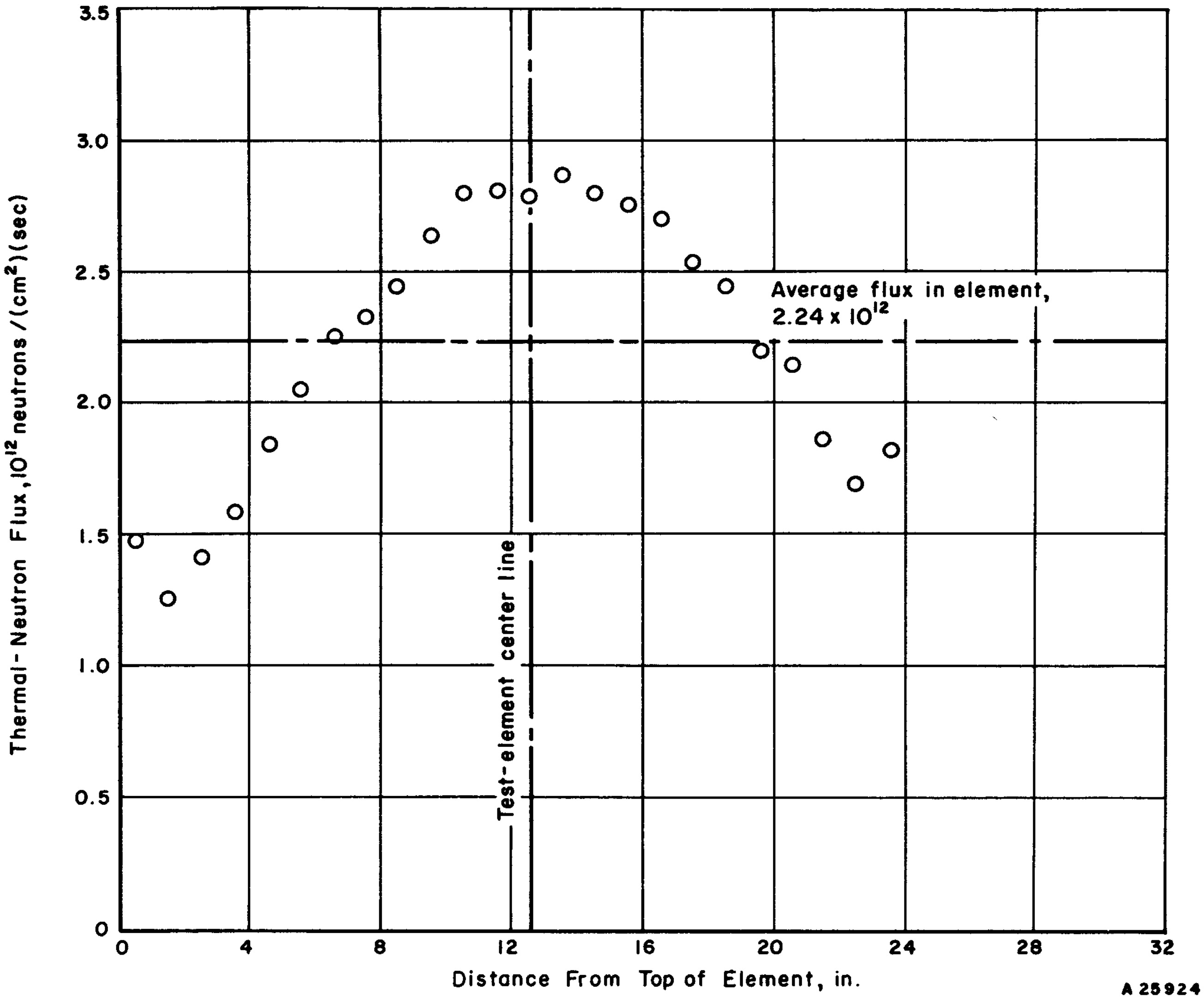

FIGURE 16. AVERAGE THERMAL-NEUTRON FLUX OVER EACH HORIZONTAL CROSS SECTION VERSUS LOCATION IN ELEMENT, SERIES II

TABLE 5. THERMAL-NEUTRON-FLUX DATA FOR APB LOOP AT ZERO-DEG ORIENTATION, SERIES III

Cross Section Number, N[a]	Thermal-Neutron Flux, 10^{12} neutrons/(cm^2)(sec), for Indicated Wire Numbers (See Figure 11)						
	1	2	3	4	5	6	7
1	2.01	1.96	2.46	2.18	2.01	2.35	2.23
2	2.01	1.90	2.29	2.12	1.56	2.23	2.07
3	2.29	2.24	2.63	2.51	1.84	2.46	2.35
4	2.68	2.57	2.98	2.85	2.07	2.96	2.68
5	3.02	3.07	3.52	3.63	2.46	3.35	3.19
6	3.46	3.41	4.08	3.57	2.85	3.74	3.63
7	5.19	3.80	4.53	3.97	3.19	4.08	4.03
8	5.87	4.24	4.97	4.13	3.46	4.64	4.58
9	--	4.75	5.25	4.52	3.63	5.03	4.92
10	--	5.08	5.81	4.92	3.91	5.31	5.42
11	5.65	5.37	6.26	5.19	4.25	5.42	5.59
12	5.92	5.70	6.38	5.37	4.25	5.70	5.70
13	6.26	5.81	6.82	5.47	4.49	5.93	5.70
14	6.37	6.26	6.93	5.69	4.64	5.93	5.70
15	6.53	6.21	6.88	5.42	4.64	6.03	5.59
16	6.65	6.32	6.99	5.81	4.97	5.93	5.87
17	6.65	6.09	6.88	5.81	4.75	5.87	7.66
18	6.37	6.03	6.82	5.64	4.53	5.87	7.38
19	6.21	5.76	6.42	5.08	4.41	5.53	5.92
20	5.76	5.47	6.14	5.08	4.13	5.48	4.86
21	5.31	5.08	5.92	4.81	3.80	5.08	4.64
22	4.81	4.58	5.37	4.36	3.58	4.64	4.47
23	4.47	4.19	4.81	4.08	3.13	4.19	4.02
24	4.36	4.30	4.97	4.36	3.85	4.97	4.64

TABLE 5. (Continued)

Cross Section Number, N[a]	Thermal-Neutron Flux, 10^{12} neutrons/(cm^2)(sec), for Indicated Wire Numbers (See Figure 11)						
	8	9	10	11	12	13	14
1	1.96	2.29	2.13	1.73	2.18	2.07	1.79
2	1.62	2.07	1.96	--	2.01	1.90	1.23
3	1.84	2.29	2.29	1.45	1.96	2.19	1.40
4	2.12	2.79	2.63	1.57	2.57	2.57	1.62
5	2.40	3.13	2.96	1.85	2.96	2.96	1.84
6	2.57	3.41	3.41	2.13	3.35	3.41	2.12
7	2.91	3.91	3.91	2.40	3.79	3.46	2.34
8	3.02	4.25	4.13	2.51	4.08	4.13	2.62
9	3.41	4.47	4.53	2.74	4.36	4.36	2.79
10	3.46	4.69	4.92	3.07	4.74	4.69	3.01
11	3.63	5.09	5.09	3.19	4.86	5.08	3.18
12	3.85	5.14	5.42	3.29	5.14	4.97	3.35
13	3.91	5.38	5.59	3.48	5.18	5.12	3.46
14	3.85	5.59	5.64	3.63	5.37	5.25	3.46
15	4.08	5.42	5.59	3.52	5.24	5.30	3.57
16	3.97	5.70	5.81	3.63	--	4.80	3.63
17	3.85	5.48	5.76	3.57	5.42	5.08	3.35
18	3.52	5.42	5.48	3.57	5.42	4.86	3.52
19	3.35	5.03	5.25	3.35	4.69	4.63	3.35
20	3.29	4.92	5.08	3.07	4.47	4.69	3.07
21	3.07	4.47	4.81	2.96	4.08	4.13	2.85
22	2.96	4.02	4.30	2.68	3.79	3.91	2.62
23	2.74	3.69	4.08	2.40	3.52	3.79	2.40
24	3.24	4.13	4.19	2.79	3.85	4.13	3.07

TABLE 5. (Continued)

Cross Section Number, N[a]	Thermal-Neutron Flux, 10^{12} neutrons/(cm^2)(sec), for Indicated Wire Numbers (See Figure 11)						
	15	16	17	18	19	20	21
1	2.12	2.23	1.73	2.12	2.24	1.90	2.23
2	1.68	2.07	1.34	2.07	2.29	1.51	2.12
3	1.96	2.35	1.51	2.35	2.46	--	2.51
4	2.40	2.85	1.79	2.57	2.96	2.12	2.73
5	2.79	4.19	2.07	2.90	3.35	2.23	3.13
6	3.07	3.85	2.29	3.46	3.69	2.57	3.52
7	3.41	4.02	2.34	3.74	4.47	5.96	3.69
8	3.69	4.30	2.68	3.85	4.74	3.35	4.47
9	4.02	4.74	3.01	4.36	4.86	3.46	4.36
10	4.24	5.02	3.18	4.52	5.59	3.79	4.80
11	4.47	5.42	3.35	4.58	5.81	3.91	5.08
12	4.41	5.47	3.46	4.97	6.14	4.07	5.19
13	4.62	5.59	3.77	5.21	6.31	4.30	5.44
14	4.92	5.81	3.80	5.19	5.97	4.41	5.42
15	5.87	5.98	3.80	5.14	6.31	4.30	5.53
16	5.14	6.03	3.80	5.19	6.48	4.30	5.98
17	5.14	5.75	3.52	5.14	6.48	4.30	5.42
18	4.80	5.75	3.51	5.03	5.97	4.30	5.92
19	4.63	5.31	3.24	4.74	5.86	3.97	5.59
20	4.41	5.08	3.24	4.52	5.19	3.97	5.31
21	4.13	4.47	2.96	4.24	4.86	3.52	4.92
22	3.85	3.96	2.68	3.85	4.69	3.18	4.41
23	3.52	4.18	--	3.74	4.13	3.07	4.36
24	4.02	--	3.29	3.80	4.47	3.96	4.69

(a) The cross section number, N, denotes that the fluxes reported are the values measured for the range N-1 to N in. from the top of the element.

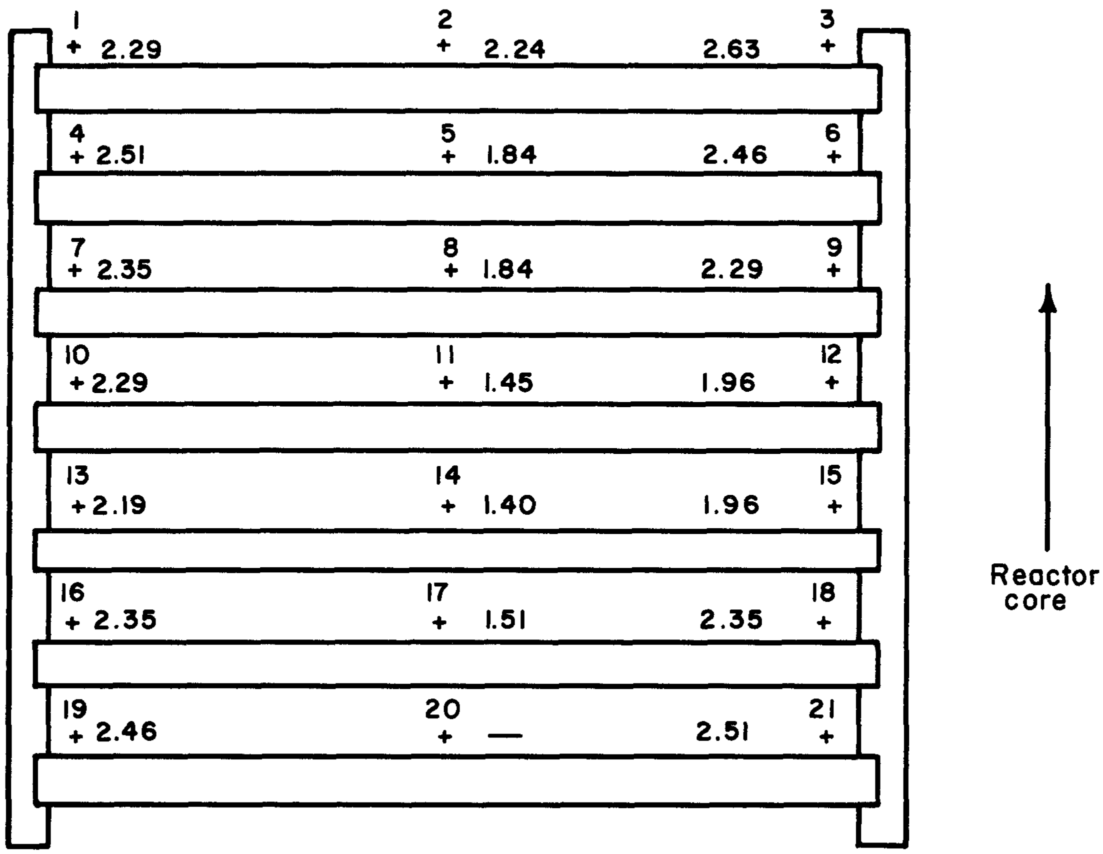

Cross-section number, N,= 3(denotes that the fluxes reported are the values measured for the range N-1 to N in. from the top of the element.)

A25925

FIGURE 17. HORIZONTAL CROSS-SECTIONAL TABULATION OF SERIES III FLUX MEASUREMENTS AT N=3 FOR APB TEST ELEMENT AT ZERO-DEG ORIENTATION

Flux values are given in terms of 10^{12} neutrons/ (cm^2) (sec).

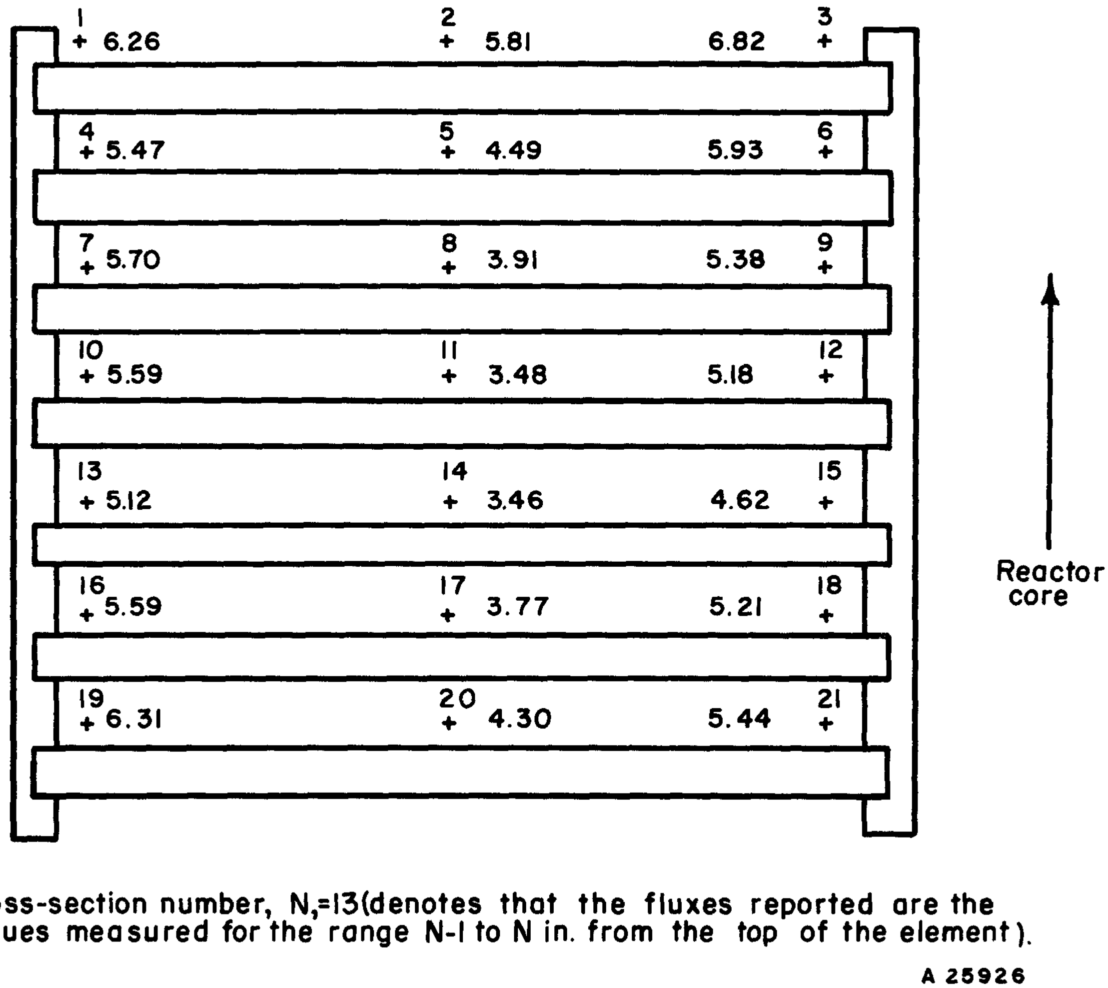

FIGURE 18. HORIZONTAL CROSS-SECTIONAL TABULATION OF SERIES III FLUX MEASUREMENTS AT N=13 FOR APB TEST ELEMENT AT ZERO-DEG ORIENTATION

Flux values are given in terms of 10^{12} neutrons/ (cm^2) (sec).

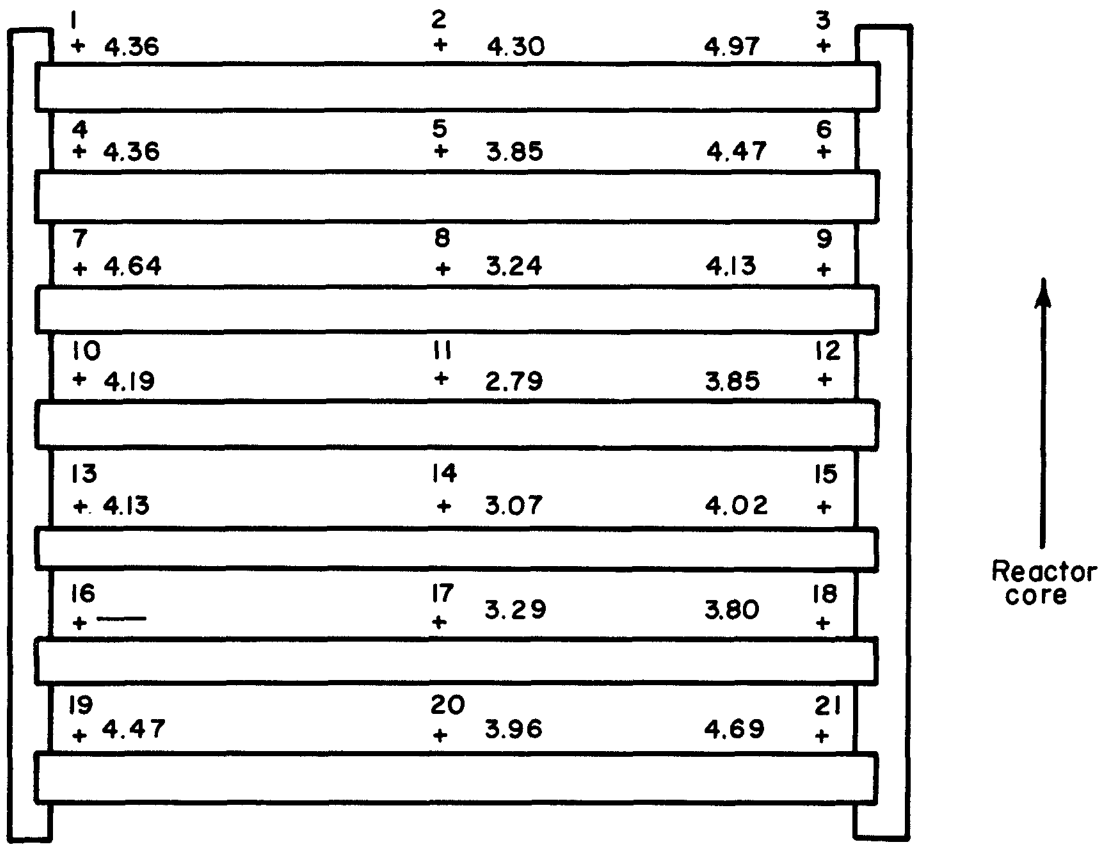

Cross-section number, N=24(denotes that the fluxes reported are the values measured for the range N-1 to N in. from the top of the element).

A 25927

FIGURE 19. HORIZONTAL CROSS-SECTIONAL TABULATION OF SERIES III FLUX MEASUREMENTS AT N=24 FOR APB TEST ELEMENT AT ZERO-DEG ORIENTATION

Flux values are given in terms of 10^{12} neutrons/ (cm^2) (sec).

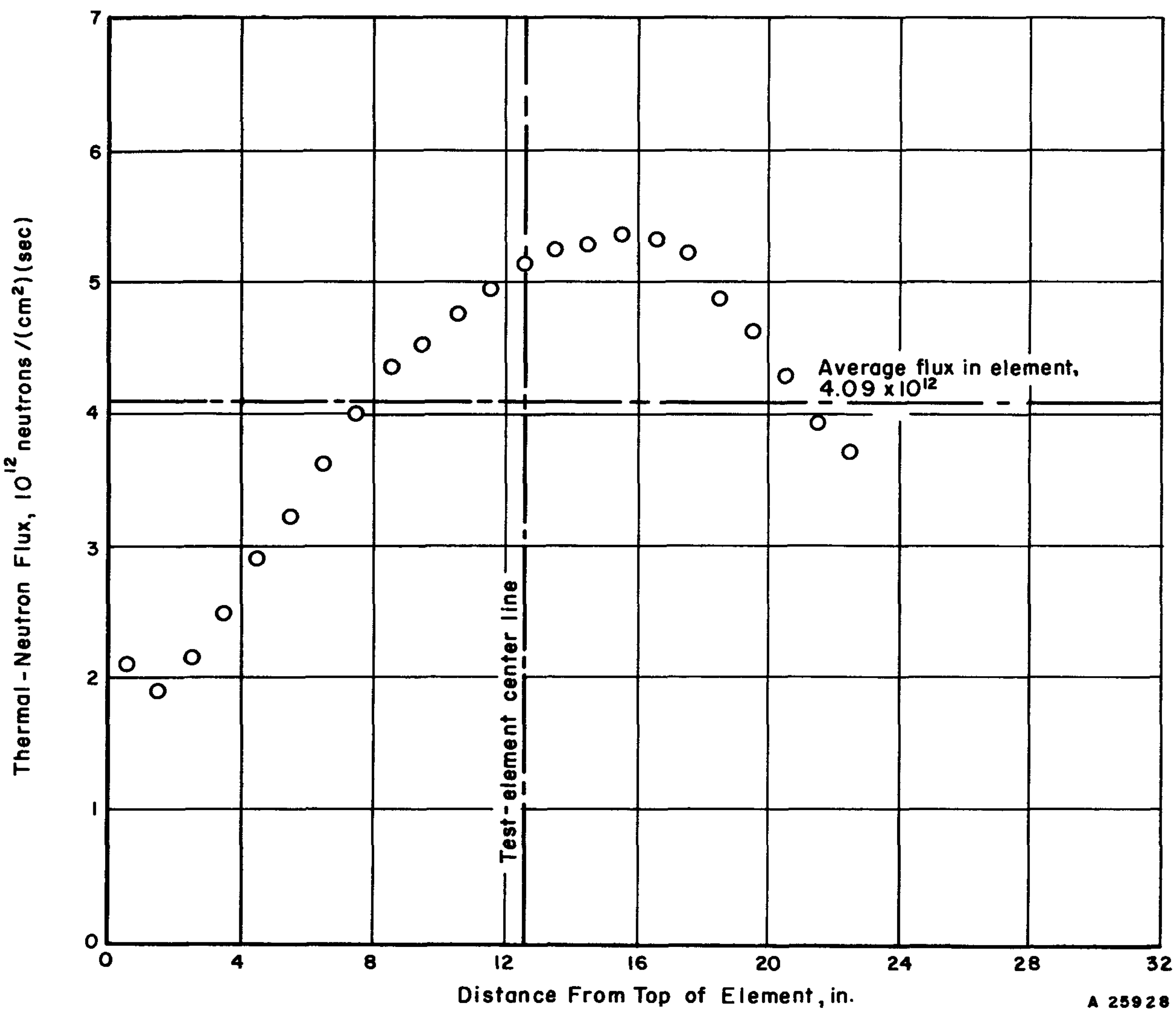

FIGURE 20. AVERAGE THERMAL-NEUTRON FLUX OVER EACH HORIZONTAL CROSS SECTION VERSUS LOCATION IN ELEMENT, SERIES III

Zero-deg orientation.

TABLE 6. THERMAL-NEUTRON-FLUX DATA FOR APB LOOP AT 90-DEG ORIENTATION, SERIES III

Cross Section Number, N[a]	Thermal-Neutron Flux, 10^{12} neutrons/(cm^2)(sec), for Indicated Wire Numbers (See Figure 11)						
	1	2	3	4	5	6	7
1	2.90	2.40	2.61	2.64	2.44	2.42	2.55
2	2.88	2.33	2.67	2.54	1.73	2.10	2.18
3	3.17	2.70	3.17	2.92	1.98	2.56	2.59
4	3.65	2.96	3.56	3.31	2.25	2.73	2.97
5	4.11	3.50	4.03	4.04	2.63	3.18	3.44
6	4.47	3.86	4.46	4.11	2.88	3.59	3.83
7	5.03	4.23	4.80	4.56	2.45	3.84	4.23
8	5.59	4.58	5.21	5.12	3.38	4.29	4.47
9	6.15	4.92	5.41	--	--	4.44	4.94
10	6.27	5.26	5.95	5.88	3.88	4.59	5.05
11	6.41	5.35	5.95	5.97	4.11	4.76	5.36
12	6.62	5.69	6.20	5.95	--	5.19	5.46
13	6.55	5.65	6.25	6.02	--	5.18	--
14	6.81	5.93	6.39	6.10	4.43	5.08	5.74
15	6.60	5.69	6.44	5.99	4.15	5.04	--
16	6.54	5.61	6.28	5.91	4.17	--	5.68
17	6.11	5.53	6.08	--	4.02	4.86	5.59
18	6.17	5.33	6.17	5.46	3.89	4.82	5.42
19	5.90	4.99	5.60	4.85	3.64	4.36	5.16
20	5.51	4.77	4.95	4.73	3.27	--	4.75
21	5.25	4.46	4.89	4.50	3.13	3.89	4.40
22	4.93	3.97	--	4.45	2.82	3.51	4.04
23	4.41	4.03	5.73	3.87	2.51	3.12	--
24	4.29	3.89	3.99	4.34	3.50	3.55	4.10

TABLE 6. (Continued)

Cross Section Number, N[a]	Thermal-Neutron Flux, 10^{12} neutrons/(cm^2)(sec), for Indicated Wire Numbers (See Figure 11)						
	8	9	10	11	12	13	14
1	2.01	2.14	2.46	1.89	2.36	2.28	1.84
2	1.38	2.04	2.25	1.33	1.97	2.26	1.33
3	1.62	2.32	2.63	1.48	2.22	2.57	1.50
4	1.87	--	2.79	1.76	2.41	--	1.70
5	2.10	2.91	3.34	1.97	2.78	3.38	2.25
6	2.37	3.19	3.43	2.24	3.24	3.46	2.41
7	2.56	--	4.08	2.43	3.48	3.83	2.36
8	2.77	3.90	4.43	2.64	3.74	4.06	2.96
9	3.02	4.06	4.73	2.82	3.88	4.38	3.05
10	3.16	4.43	5.48	3.02	4.27	4.38	3.02
11	3.23	4.47	5.72	3.12	4.26	4.92	3.13
12	3.39	4.49	5.40	3.16	4.34	5.13	3.18
13	3.71	4.66	5.54	3.14	4.33	5.22	3.26
14	3.69	4.28	5.63	--	4.46	5.23	3.26
15	3.46	4.51	5.58	3.25	4.46	5.17	3.19
16	--	4.54	5.62	3.17	4.30	5.42	3.11
17	3.34	4.28	5.33	3.06	4.23	5.25	2.96
18	3.33	4.12	5.60	2.89	4.07	5.15	2.82
19	3.12	3.93	4.81	2.72	3.80	4.89	2.66
20	2.88	3.62	4.45	2.56	3.65	4.66	2.38
21	2.60	3.58	--	2.39	3.36	4.31	2.22
22	2.14	3.15	3.82	2.20	3.06	4.21	1.97
23	2.71	2.84	3.42	1.97	2.77	3.67	1.91
24	--	3.25	3.78	2.70	2.78	3.70	2.52

TABLE 6. (Continued)

Cross Section Number, N[a]	Thermal-Neutron Flux, 10^{12} neutrons/(cm^2)(sec), for Indicated Wire Numbers (See Figure 11)						
	15	16	17	18	19	20	21
1	2.24	2.64	2.03	2.30	2.64	2.11	2.40
2	2.10	2.36	1.46	--	2.54	1.78	2.27
3	2.28	2.68	1.67	2.45	2.89	1.99	2.61
4	2.61	3.07	1.90	2.82	3.44	2.28	3.02
5	2.93	3.49	2.10	3.09	3.73	2.60	3.41
6	3.17	4.05	2.43	3.52	4.20	2.99	3.93
7	3.44	4.19	2.66	3.80	4.58	3.27	4.21
8	3.73	4.83	2.87	4.01	5.07	3.48	4.83
9	4.03	4.93	3.04	4.27	5.37	3.76	4.90
10	4.14	4.99	3.20	4.61	5.55	4.03	5.11
11	4.28	5.35	3.31	4.81	5.84	4.18	5.39
12	4.33	5.71	3.46	4.80	5.89	4.38	5.34
13	4.53	5.66	3.43	4.81	6.07	4.44	5.57
14	4.60	5.64	3.74	4.93	6.05	4.29	5.78
15	4.49	5.54	3.43	4.79	6.11	--	5.72
16	4.46	5.66	3.37	4.78	6.10	4.43	5.78
17	4.18	5.56	3.35	4.69	--	4.42	5.29
18	4.01	5.28	3.19	4.49	5.48	4.04	5.23
19	3.68	4.95	2.98	4.34	5.33	3.80	4.85
20	3.51	4.56	2.92	4.01	5.19	3.48	4.52
21	3.25	4.33	2.63	3.59	4.71	3.27	4.36
22	2.79	4.19	2.36	3.24	4.45	3.08	3.84
23	2.61	3.50	2.17	3.13	4.07	2.71	3.40
24	3.00	4.00	2.60	3.25	4.38	2.99	3.40

(a) The cross section number, N, denotes that the fluxes reported are the values measured for the range N-1 to N in. from the top of the element.

TABLE 7. SPECIFIC ACTIVITIES OF SEGMENTS OF GOLD FOILS LOCATED ON THE SURFACE OF FUEL PLATES OF THE MARK I TEST ELEMENT

	Foil 1		Foil 2		Foil 3		Foil 4		Foil 5		Foil 6	
Segment	A	X, in.	A	X, in.	A	X, in.	A	X, in.	A	X, in.	A	X, in.
1	4.63	0.0805	7.67	0.0670	5.60	0.0853	3.41	0.0873	5.82	0.0624	4.80	0.0554
2	4.51	0.1445	7.64	0.1183	5.41	0.1298	2.94	0.1392	5.10	0.1230	4.23	0.1073
3	4.15	0.2128	6.75	0.1970	5.82	0.1922	--	0.1995	4.84	0.1834	4.11	0.1681
4	4.17	0.2805	6.77	0.2549	5.46	0.2626	--	0.2456	4.82	0.2471	4.15	0.2280
5	4.07	0.3366	--	0.3249	--	0.3030	--	0.2835	4.72	0.3214	3.80	0.2730
6	3.86	0.4137	--	0.3866	5.33	0.3699	2.74	0.3363	4.52	0.3853	3.71	0.3109
7	3.55	0.4649	6.55	0.4476	5.56	0.4143	2.68	0.4306	4.30	0.4453	3.28	0.3409
8	3.79	0.5284	6.34	0.5164	5.26	0.4655	2.92	0.5106	4.40	0.4896	3.68	0.3912
9	3.77	0.5865	6.41	0.5818	5.12	0.5181	2.66	0.5849	4.33	0.5472	3.86	0.4460
10	3.59	0.6639	6.53	0.6371	5.41	0.5976	2.60	0.6449	4.47	0.5894	3.44	0.4829
11	3.98	0.7491	6.51	0.7148	5.35	0.6639	2.66	0.6887	4.27	0.6501	3.63	0.5424
12	3.97	0.7942	6.91	0.7536	5.37	0.7133	2.73	0.7677	4.36	0.6962	--	0.6121
13	3.80	0.8421	6.60	0.8187	--	0.7682	2.73	0.8337	4.41	0.7418	3.62	0.6756
14	3.90	0.8923	6.91	0.8724	5.61	0.8375	2.57	0.8897	4.37	0.7843	3.87	0.7528
15	4.00	0.9424	6.68	0.9172	5.76	0.8867	2.71	0.9450	4.42	0.8308	3.73	0.8288
16	4.07	1.0091	6.83	0.9724	5.98	0.9360	3.04	0.9975	4.44	0.8878	3.97	0.8972
17	4.03	1.0497	6.32	1.0314	--	0.9990	--	--	4.57	0.9307	3.94	0.9592
18	4.21	1.1130	7.25	1.0929	--	--	--	--	4.94	1.0055	4.23	1.0598
19	--	--	--	--	--	--	--	--	5.90	1.0677	--	--

Note:

(1) A is the specific activity of the foil segment (arbitrary units).

(2) X is the distance from the inner face of the side plate to the far extremity of the particular segment. The width of a particular segment can be found by subtracting from X the distance of the preceding segment.

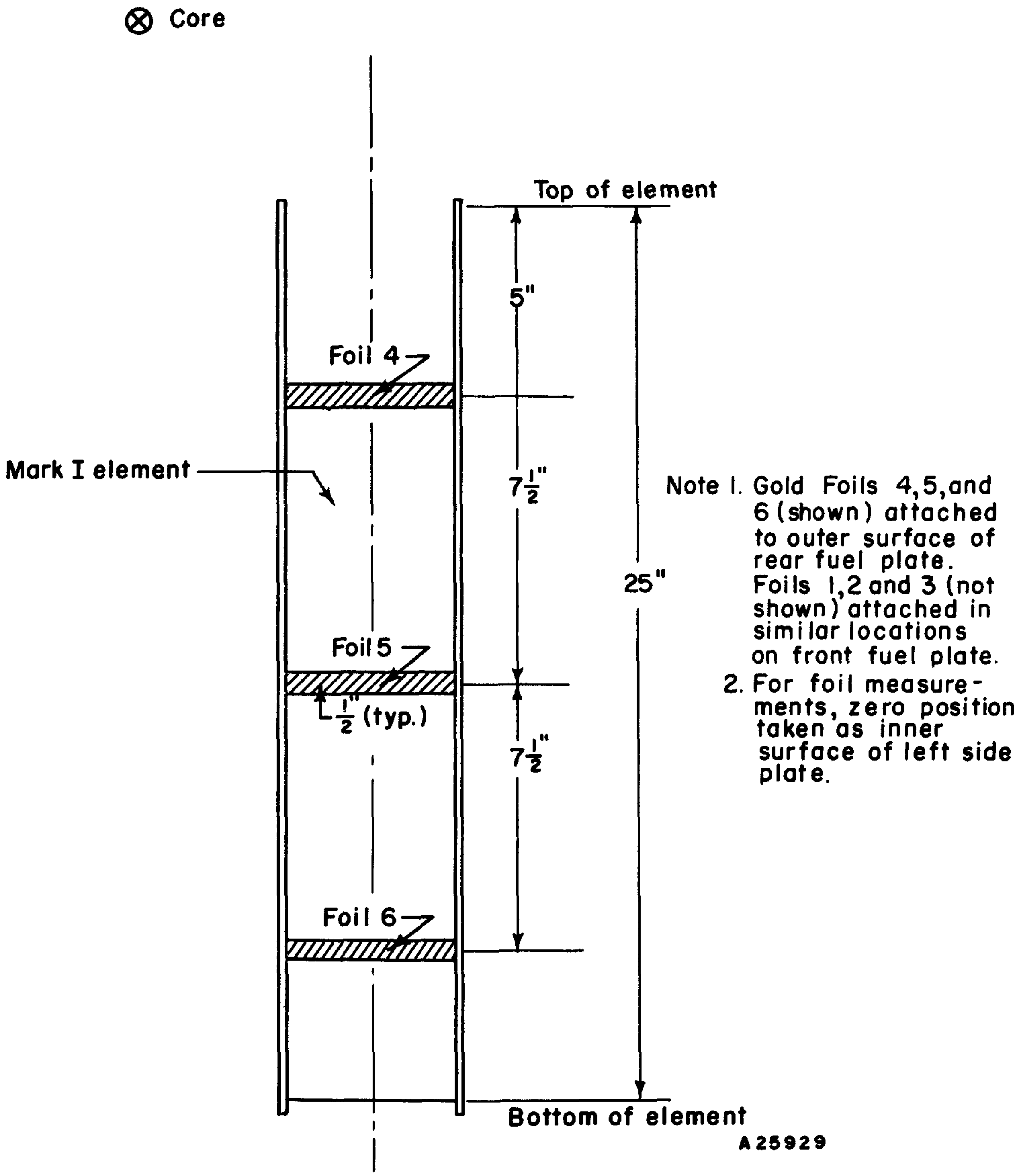

FIGURE 21. LOCATIONS OF GOLD FOIL IN MARK I ELEMENT

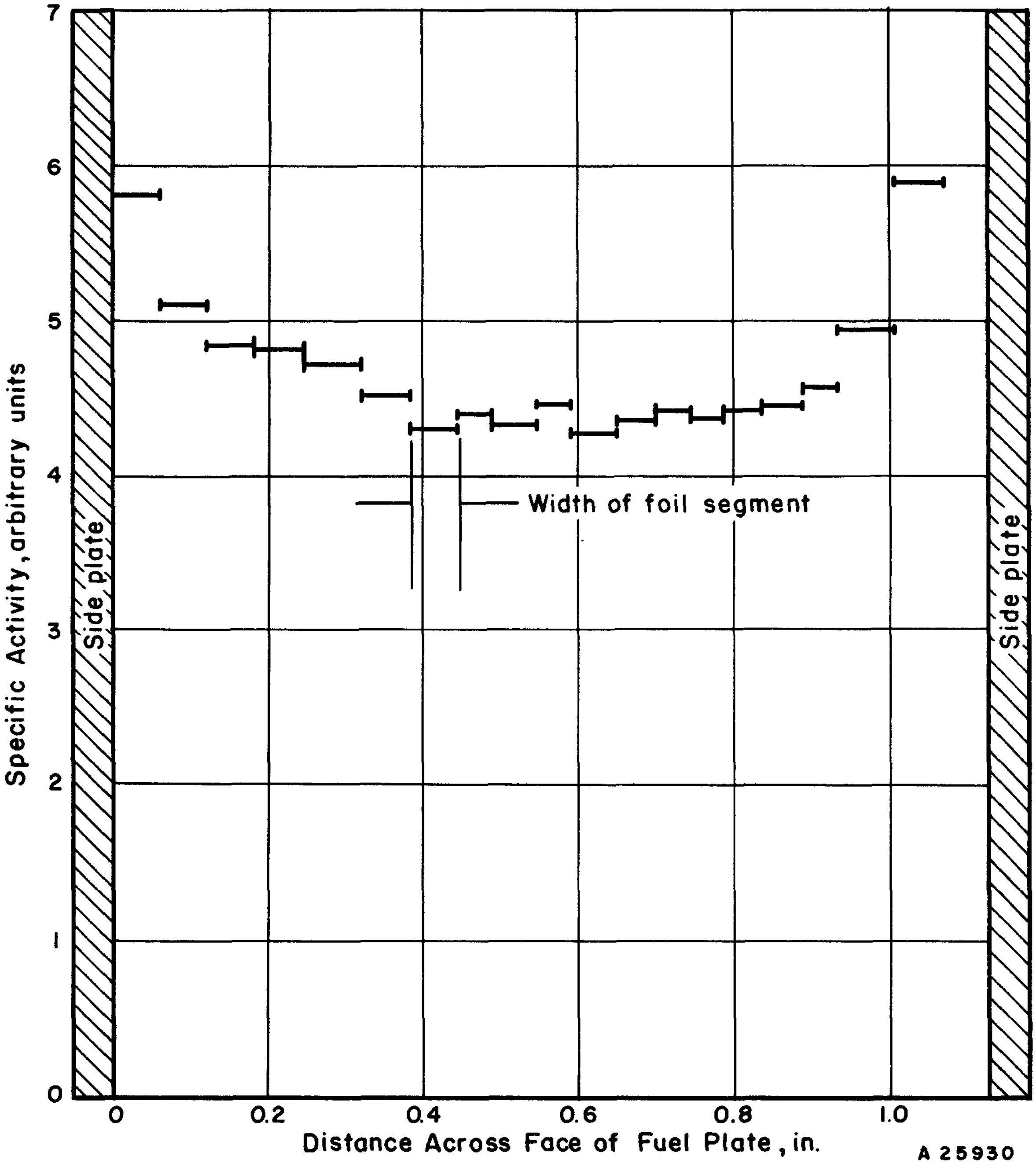

FIGURE 22. SPECIFIC ACTIVITY OF FOIL 5 SEGMENTS VERSUS LOCATION ON FUEL PLATE

the positive reactivity contribution of the fuel element to the core is offset by the negative reactivity effect of the loop void in the reflector of the core.

Subsequent flooding of the loop with water with the fuel element in place revealed a positive reactivity contribution of the test element of only 0.0009 $\frac{\Delta k_{eff}}{k_{eff}}$.

DISCUSSION OF THE ACCURACY OF THE MEASUREMENTS

The error associated with the absolute thermal-neutron-flux determination has been estimated as within ±10 per cent. The principal contribution to this error is the precision of the counter standardization. The activity of the standard cesium source is known to ±3 per cent. Counting statistics and the deduction of the areas under the photopeaks contribute another 2 per cent, so that the gross error assigned to counter standardization is ±5 per cent. In the conversion of foil activity into flux, the accuracy of the thermal-neutron cross section of gold, foil weight, and time measurements must be considered. It was estimated that these sources contribute approximately 2 per cent error. Errors involved in positioning of the wires and foils, normalization of the wire activity to the foil-determined flux, and measurement of the cadmium ratio contribute 2 to 3 per cent, bringing the total estimated error up to ±10 per cent.

The above discussion of experimental error applies strictly to only the flux distribution measurements made with the manganese-iron wires and gold foils.

SUMMARY

The loop and core arrangement shown in Figure 9 has been chosen for the initial in-pile loop operation. With this arrangement, it is possible to obtain an average flux of 4.09×10^{12} neutrons/(cm^2)(sec) with a corresponding power generation of approximately 45 kw. Lower powers can be attained by moving the loop from the core. The peak thermal flux is a factor of 1.87 above the average flux and the general flux depression from the edge of the element to the center is a factor of two or less.

WRM:JNA:JWC/bas